THESIS

CHARACTERIZATION OF THE SELECTIVE HYDROLYSIS OF BRANCHED UBIQUITIN CHAINS BY UCH37 AND ITS ACTIVATOR RPN13

Submitted by

Zachary S Hazlett

Department of Biochemistry and Molecular Biology

In partial fulfillment of the requirements

For the Degree of Master of Science

Colorado State University

Fort Collins, Colorado

Fall 2020

Master's Committee:

Advisor: Tingting Yao

Robert Cohen
Olve Peersen
Santiago DiPietro
Alan Kennan

ABSTRACT

CHARACTERIZATION OF THE SELECTIVE HYDROLYSIS OF BRANCHED UBIQUITIN CHAINS BY UCH37 AND ITS ACTIVATOR RPN13

The ubiquitin (Ub) C-terminal hydrolase, Uch37, can be found associated with the 26S proteasome as well as the INO80 chromatin remodeling complex. Bound to the 26S proteasome, it assists in regulating the degradation of Ub modified proteins. The proteasomal subunit Rpn13 binds Uch37, anchors it to the proteasome 19S regulatory particle and enhances the deubiquitinating enzyme's (DUB's) catalytic activity. While the structure of the Uch37/Rpn13 complex bound to a single Ub molecule has been characterized, much still remains unknown regarding the enzyme's substrate specificity, the molecular basis for its substrate specificity, and its function in the regulation of proteasomal degradation. In this thesis we characterize the substrate specificity of Uch37 with and without its proteasomal binding partner Rpn13. By synthesizing poly-Ub chains of various linkage types and topologies and using these Ub chains in *in vitro* deubiquitination assays, we were able to determine that Uch37/Rpn13 selectively cleaves branched Ub chains. This provides evidence to suggest that Uch37 is the first enzyme with activity specific for branched Ub chains. Branched Ub chains have been identified endogenously and have roles connected to the regulation of nascent misfolded polypeptides, cell cycle control, and the enhancement of proteasomal degradation. The work presented here sets out to characterize the molecular mechanism of branched chain hydrolysis by Uch37 and its binding partner Rpn13, determine the kinetics of this enzymatic reaction, and establish a system for probing the function of "debranching" by Uch37 in proteasomal degradation. The conclusion of our work builds our understanding of the complex system of intracellular signaling by Ub and unveils key elements to the primary system responsible for regulating cellular protein homeostasis.

TABLE OF CONTENTS

CHAPTER 1: INTRODUCTION

1.1 Ub and the complexity of the Ub code

Ubiquitin (Ub) is a small 8.6 kDa protein distributed ubiquitously throughout most of the eukaryotic cell and is found among all tissue types. Ubiquitination enzymes, composed of Ub activating (E1), Ub conjugating (E2), and Ub ligating enzymes (E3), sequentially catalyze the reactions necessary to covalently attach the carboxy-terminus of Ub to primary amines of proteins primarily at lysine amino acid residues. Proteins can be monoubiquitinated, i.e., modified at one or more locations with a single Ub, or polyubiquitinated, modified at one or more locations by a covalently linked chain of multiple Ub molecules. Ub contains seven lysine residues and an N-terminal amine, which serve as eight potential positions for the attachment of another Ub molecule (FIG 1.1, A). This characteristic of Ub combined with the large assortment of Ub conjugating enzymes able to generate different linkage types produces the possibility for many types of poly-Ub chains that can be generated in the cell. Poly-Ub can be built in homotypic chains containing a single type of Ub–Ub linkage, or heterotypic chains consisting of two or more different Ub linkage types in the same poly-Ub chain. Heterotypic chains can be either linear in their linkages, or exist as branched chains, where one proximal Ub serves as the acceptor for two distally linked donor Ub molecules at two separate positions. Different Ub–Ub linkage types have been found to be associated with distinct structures. For example, NMR studies have revealed that di-Ub linked at K48 predominately exists in the “closed” conformation under physiological conditions.[3] This conformation involves a thermodynamically favorable interaction between the hydrophobic patches (L8, I44, V70) of both the proximal and distal Ub in a K48-linked Ub dimer. In contrast, crystal structures of K63 linked Ub chains have revealed that this linkage favors a fully extended “open” conformation.[4] As the downstream fate of the protein is dependent on the type of Ub modification and the effectors specific for various linkage types and chain topologies, it is easy to see that ubiquitination serves as a complex form of signaling within the cell.

A

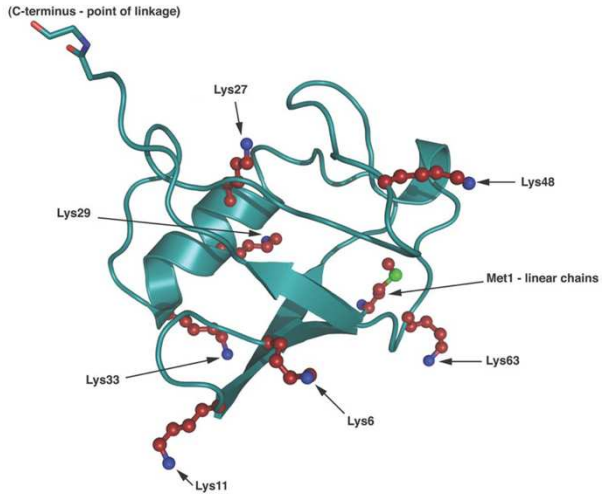

B

Linear Chains	6 Ub–^{6}Ub	48 Ub–^{48}Ub		
	6 6 Ub–^{6}Ub–^{6}Ub	11 11 Ub–^{11}Ub–^{11}Ub	48 48 Ub–^{48}Ub–^{48}Ub	63 63 Ub–^{63}Ub–^{63}Ub
	6 48 Ub–^{6}Ub–^{48}Ub	48 6 Ub–^{48}Ub–^{6}Ub		
Branched Chains	6 48 [Ub]$_2$–^{6,48}Ub	11 48 [Ub]$_2$–^{11,48}Ub	63 48 [Ub]$_2$–^{48,63}Ub	

FIG 1.1 Ubiquitin structure and the linear and branched Ub chains generated to determine the substrate specificity and catalytic activity of Uch37/Rpn13. (A) Model of ubiquitin adapted from Komander D. et al. (2009) indicating all eight potential points of Ub conjugation and the C-terminus.[2] (B) Homotypic chains are those containing a single Ub–Ub linkage type and heterotypic are those containing more than one Ub–Ub linkage type.

With the abundance of protein ubiquitination, the significant roles these events play in major cellular pathways, and the pathologies associated with aberrations in these pathways such as cancer and neurodegenerative diseases,[5] it behooves us to understand the chemical and molecular basis for the various ubiquitin dependent regulatory mechanisms.

For the purposes of discussion in this text, we have adopted the nomenclature of poly-Ub chains from the Fushman Lab outlined in Boughton et al. 2019.[6] Each poly Ub chain of defined length and linkage type will be denoted from the left to right as the distal Ub to the proximal Ub. Ub to Ub linkage will be denoted as Ub–Ub with the position of linkage identified at the proximal Ub (example: Ub–^{48}Ub). Branched chains will be identified as two distal ubiquitins linked at two different positions on the proximal Ub (example: $[Ub]_2$–^{6,48}Ub). FIG 1.1, B presents each di- and tri-Ub we synthesized and how it will be referred to throughout this text.

1.2 Uncovering the function of branched Ub chains

Individual Ub–Ub linkage types have been found to be associated with distinct cell signaling pathways. For example, the K48 linkage serves as the primary poly-Ub signal for proteasome mediated substrate degradation, where the K63 linkage is associated with endocytosis and intracellular trafficking.[7, 8]

The branched ubiquitin chain as a unique signal within the cell is just recently being uncovered. Early studies first identified that branched Ub chains could be generated using the certain combinations of Ub conjugating enzymes.[9] Using various E3 ligases (CHIP, MuRF1, or Mdm2) with the E2 UbcH5, polyUb chains were generated, digested with trypsin, and subject to tandem mass spectrometry. As trypsin digest of Ub produces a diglycine remnant from cleaving C-terminal to R74 at the Ub C-terminus, the digest of poly-Ub produces Ub peptides linked with diGly at their positions of Ub conjugation. The identification of two diGly remnants on a single peptide via mass spectrometry analysis provided one of the first indications that Ub could be conjugated in a branched chain topology.

Later studies out of the Rape lab at Berkeley proceeded to further characterize the functional significance of branched Ub chains by analyzing the anaphase promoting complex (APC/C), a mitotic regulator and Ub E3 ligase.[10] Using *in vitro* ubiquitination assays with K11 Ub (a single Lys mutant of Ub), and K11R Ub (single Lys to Arg mutant of Ub), it was discovered that the APC/C builds mixed linkage chains that are distinct from linear heterotypic chains. Using substrates containing pre-existing linear Ub chains of defined lengths and incubating with methylated Ub (a Ub monomer that can only act as a donor) the APC/C along with its E2 Ube2S, was confirmed to conjugate branched Ub chain linkages. Using a different type of Ub mutant, these researches sought to detect branched Ub chains produced by the APC/C within the cell. HeLa cells were transfected with a gene construct for Ub that contained an internal TEV cleavage site and FLAG epitope. Expression of this Ub, immunoprecipitation of various cell cycle regulators during early mitosis, followed by TEV cleavage and western blot analysis allowed for the visual detection of evidence for branched chain formation based on the number of FLAG epitopes remaining after cleavage. This process along with the use of inhibitors for APC/C allowed for the determination that the APC/C functions to generate branched Ub chains for the purpose of regulating the cell-cycle during early mitosis. The same study tracked the proteasomal degradation of branched chain versus linear chain modified substrates (cell-cycle regulators) to reveal that branched Ub chains enhance the proteasomal degradation of modified substrates.

Years later, the same lab was able to produce an antibody specific for the K11/K48 branched Ub chain linkage to show that the APC/C regulatory function described earlier specifically involves the enzyme's ability to conjugate K11/K48-linked branched chains.[11] This "bi-specific" antibody allowed for the detection of K11/K48-linked branched chains in 293T cells in response to proteotoxic stress. IP of branched chains using this antibody followed by mass spectrometry allowed for the identification of other enzymes/effectors related to this Ub chain type. This and a number of other biochemical assays revealed that the E3 ligases Ubr4 and

Ubr5 are two enzymes responsible for generating the majority of K11/K48-linkages during proteotoxic stress, specifically mediating the proteasomal degradation of nascent misfolded polypeptides.

Other studies have linked specific functions in the cell to other distinct branched Ub chain linkage types. In 2017, Ufd2p was discovered to have the ability to conjugate Ub at K48 onto pre-existing K29-linked poly Ub chains for the purpose of converting this Ub modification into one able to shuttle the target protein to the proteasome for degradation.[12] This study revealed that this type of Ub signal conversion is essential for the ER-associated degradation pathway. Another study revealed that K48/K63-linked branched Ub chains enhance NFkB singling during the innate and adaptive immune response.[13]

With eight possible linkage types, there are 28 possible branched Ub chains composed of two linkage types, and larger numbers of possible branched chains including those containing three or more linkages. The findings described above reveal that these Ub chain types can relay unique signals oftentimes more than the sum of their individual linkage types. Due to these facts, it is clear that there is still much to learn about the importance of branched chain signaling within the cell. Importantly, the characterization of enzymes that recognize and act upon branched Ub chains remains poorly understood. In the study presented in this thesis, we characterize one of the first deubiquitinating enzymes identified to possesses branched chain specific activity, the proteasomal DUB Uch37.

1.3 Ubiquitination functions in regulating substrate degradation by the proteasome

One of the primary systems responsible for the maintenance of protein homeostasis (also known as “proteostasis”) is the ubiquitin proteasome system (UPS). The 26S proteasome is a 2.5 MDa protein complex responsible for the majority of the protein degradation within the cell.[14] It is composed of a cylindrical 20S proteolytic chamber, or core particle (CP), capped on one or both ends by 19S regulatory particles (RPs) (FIG 1.2, A).[15] The 19S regulatory particle is comprised of a lid and base subcomplex.[16] A hexameric AAA-ATPase ring exists as a

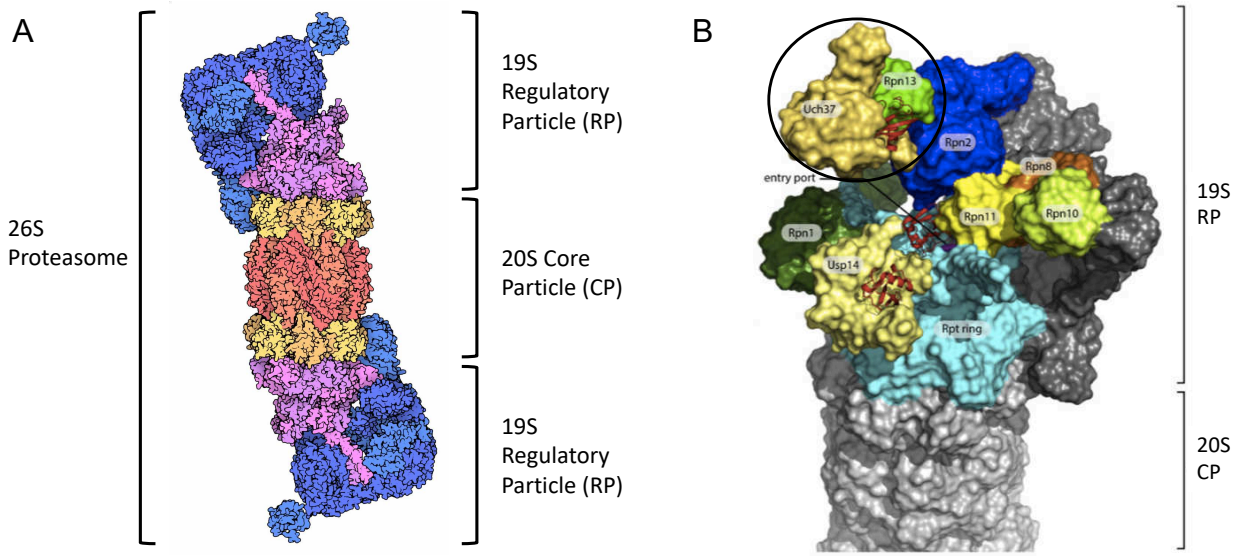

FIG 1.2 The structure of the 26S Proteasome and the composition of the 19S regulatory particle. (A) Model of the 26S proteasome adapted from the EM Data Bank: *EMD-2165*. The 20S core particle (orange and yellow) is flanked by two 19S regulatory particles (pink and blue). (B) Model of the 26S proteasome adapted from de Poot S.A.H. et al. (2017).[1] Components of the 19S regulatory particle are identified along with the entry port where unfolding polypeptides are translocated into the 20S degradative core particle. The position of Uch37 and Rpn13 at the 19S RP is circled for emphasis.

component of the base and is responsible for unfolding polypeptides and translocating them into the 20S degradative chamber. The lid complex is made up of a variety of different components including Ub receptors and deubiquitinating enzymes that serve to regulate proteasome function. For a protein to be degraded by the proteasome, it is first ubiquitinated in a stepwise reaction carried out by Ub activating (E1), Ub conjugating (E2), and Ub ligating (E3) enzymes. The Ub-modified protein either binds directly to 19S Ub receptors or is shuttled to the proteasome by Ub-binding shuttles/chaperones.[17, 18] Once bound, an unstructured initiation region of the protein must engage with the pore loops of the proteasome AAA-ATPases, then using the power from the hydrolysis of ATP, the proteasome unfolds the protein while threading it into the degradative chamber. Before and during unfolding and translocation, the protein is deubiquitinated by proteasome associated deubiquitinating enzymes and Ub is recycled. Finally, the unfolded polypeptide reaches the proteolytic sites residing in the center of the 20S core and the protein is degraded.

1.4 Uch37 and its connection to the UPS

The many components of the 26S proteasome work together to maintain the tight regulation of proteasomal degradation. One key element of degradation regulation is the activities of the three proteasome-associated deubiquitinating enzymes (DUBs) Rpn11, Usp14, and Uch37 located at the 19S RP (FIG 1.2, B).[1] Rpn11 has been identified as an essential component of proteasomal degradation. Rpn11 resides just above the 19S entry channel, and deubiquitinates mono-Ub and poly-Ub *en bloc* (or all at once) as unfolding polypeptides are threaded into the 20S core particle.[19] Without this *en bloc* DUB activity, a translocating polypeptide still modified with Ub will become stalled at the entry port. Drugs such as O-phenanthroline have been used to inhibit Rpn11, leading to the full inhibition of proteasomal function as a means of therapeutic treatment for multiple myeloma.[20] Positioned further from the entry channel, Usp14 also deubiquitinates Ub and poly-Ub from substrates *en bloc*, until a single Ub chain remains.[21] This activity has been shown to reduce the dwell time of ubiquitinated substrates at the proteasome leading to diminished proteasomal degradation. Studies of the yeast ortholog of Usp14, Ubp6, has revealed a second non-catalytic function of this DUB. The Ub and proteasome-bound Ubp6 has been shown to alter the conformational state of the proteasome, stabilizing it in the substrate-engaged conformation, leading to a diminished ability for the proteasome to engage subsequent substrates.[22] While the function of Rpn11 and Usp14 have been fairly well characterized, much regarding the regulatory contribution of Uch37 toward substrate degradation and proteasome regulation remains unknown.

Uch37 is a highly conserved DUB of the Ub C-terminal Hydrolase family. The enzyme's catalytic active site cysteine is found within the UCH domain ($Uch37^{UCH}$). A 21-amino acid unstructured region known as the "Active Site Crossover Loop (ASCL)" sterically regulates access of substrates to the active site. The C-terminal domain ($Uch37^{CTD}$) is made up of four α-helices that can be bound by Rpn13 or NFRKB, recruiting Uch37 to the proteasome or INO80

complex, respectively. Binding by Rpn13, a component of the 19S RP, has been shown to stabilize the ASCL and increase DUB activity toward small Ub adducts.[23] Binding by NFRKB inhibits Uch37 DUB activity. The function of Uch37 in the INO80 chromatin remodeling complex remains unknown.[23]

Uch37 has been identified as an essential regulator of cell cycle progression and has been implicated in esophageal, hepatocellular, and ovarian tumor progression as its expression levels are higher in these malignant tissue types relative to non-cancerous tissue.[24-26] Uch37 as well as Usp14, Rpn11, and the 20S core proteasome have been extensively investigated as therapeutic targets for the treatment of various cancer types.[27] This highlights the importance of understanding the function and molecular basis of regulation of Uch37 at the proteasome.

In this paper, we characterize the enzymatic activity of Uch37 while establishing the components necessary to probe the function of Uch37 at the proteasome. Using *in vitro* deubiquitination assays with recombinantly purified enzymes and poly-Ub chains of distinct lengths, linkage types, and topologies, we were able to reveal Uch37 substrate specificity for branched Ub chains. From this arises a number of important questions: How does the proteasome subunit and Uch37 binding partner Rpn13 modulate this DUB's substrate specificity? What structural features of the enzyme and the substrate are required for branched Ub chain specificity? What are the kinetics of branched chain deubiquitination or "debranching" by Uch37/Rpn13? And how might this unique type of enzymatic activity affect processing of substrates by the proteasome? This thesis presents our findings that establish the molecular basis for Uch37 activity in coordination with Rpn13. From here we propose how this activity might modulate proteasome substrate degradation and outline the next steps needed to determine Uch37 function at the proteasome.

CHAPTER 2: UCH37 SUBSTRATE SPECIFICITY

2.1 Introduction

One of the first steps in understanding the function of Uch37 at the proteasome is to determine the substrate specificity of the enzyme, both alone and with its proteasome associated binding partner Rpn13. With the knowledge that Uch37 is a deubiquitinating enzyme, there are many Ub substrates that Uch37 could proteolyze. To determine which poly-Ub linkage type and/or topology might be preferred, a sampling of homotypic (single linkage type) and heterotypic (more than one linkage type) linear and branched chains were synthesized using approaches outlined in the "Controlled Synthesis of Polyubiquitin Chains."[28] FIG. 1.1, B presents each chain that was made and used in the determination of Uch37 substrate specificity. Uch37, Rpn13 full length ($Rpn13^{FL}$), and Rpn13 C-terminal domain ($Rpn13^{C}$; 285-407) were expressed and purified as described.[23] Baseline activity was measured for each enzyme complex by monitoring fluorescence increase from the hydrolysis of Ub-AMC over time (Fig 2.1). The differences in baseline activity were considered in the interpretation of later assays. Most noticeably, co-purified NS-Uch37/$Rpn13^{FL}$ is approximately half as active as Co-purified NS-Uch37/$Rpn13^{C}$, which will be addressed when used together to compare activity. As past

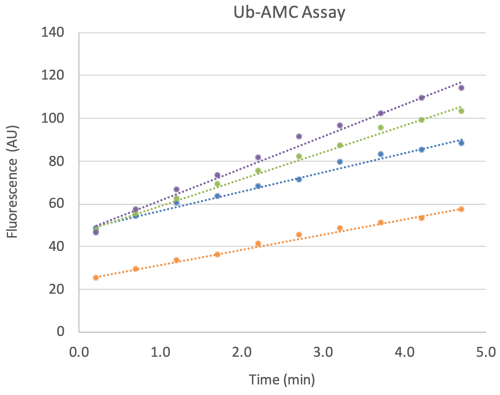

Enzymes	Slope of Ub-AMC assay (AU/min)	Activity relative to His-TEV-6A-Uch37 + Rpn13C
His-TEV-6A-Uch37 + Rpn13C	9.714	1.00
NS-Uch37 + Rpn13C	13.38	1.38
Co-purified NS-Uch37/Rpn13C	15.95	1.64
Co-purified NS-Uch37/Rpn13FL	7.571	0.78

FIG 2.1 Comparing baseline activity of each Uch37/$Rpn13^{C}$ construct by monitoring hydrolysis of Ub-AMC. Fluorescence increase due to the hydrolysis of Ub-AMC by each Uch37/$Rpn13^{C}$ construct was monitored over time. The slope of each line is presented to compare the baseline activity of each enzyme complex. Activity is shown relative to His-TEV-6A Uch37 + $Rpn13^{C}$.

studies revealed that Rpn13^{C} is sufficient for binding and activating Uch37 toward the hydrolysis of Ub-AMC, Rpn13^{C} was used in assays for Uch37 substrate binding and hydrolysis.[23, 29]

2.2 UCH37 preferentially cleaves branched Ub chains over linear Ub chains

Using an *in vitro* approach, incubating recombinant Uch37/Rpn13^{C} with each type of poly-Ub chain generated, and analyzing the reaction at distinct time points via SDS-PAGE and Coomassie stain, we were able to determine that Uch37 preferentially cleaves branched Ub chains over linear Ub chains of similar lengths and linkage types (FIG 2.2, A & B). In reactions with 10 μM Uch37/Rpn13^{C} and 5 μM linear homotypic and heterotypic Ub trimer (Ub3) chains (incubated at 37ºC for 1 hour), no more than 5% of reactant was deubiquitinated (FIG 2.2, C *left*). Under similar conditions, but with only 1 μM Uch37/Rpn13^{C}, branched Ub chains were cleaved far more abundantly than linear chains of the same linkages and number of ubiquitins (FIG 2.2, C *right*).

2.3 UCH37 exclusively cleaves the K48 linkage within K48-linkage containing branched Ub chains

From the pattern observed from branched chain deubiquitination by Uch37/Rpn13^{C}, it can be seen that upon hydrolysis of each branched Ub chain type, the products of Ub dimer (Ub2) to Ub monomer (Ub1) are produced in a 2:1 ratio (FIG 2.2, C *right*). This suggests that Uch37 cleaves branched Ub chains at only one of the two linkages. In order to determine which linkage is a preferred position of hydrolysis, the *in vitro* DUB assay was run as before, and the products were analyzed by western blot. A K48-linkage specific antibody and a K6-linkage specific affimer were used to detect substrate and product linkage types in the deubiquitination reactions against either the branched $[Ub]_2$–^{6,48}Ub or the linear Ub–^{48}Ub–^{48}Ub.[30] OTUB1, a DUB that specifically cleaves the K48 linkage,[31] was used as a control. In reactions of Uch37/Rpn13^{C}

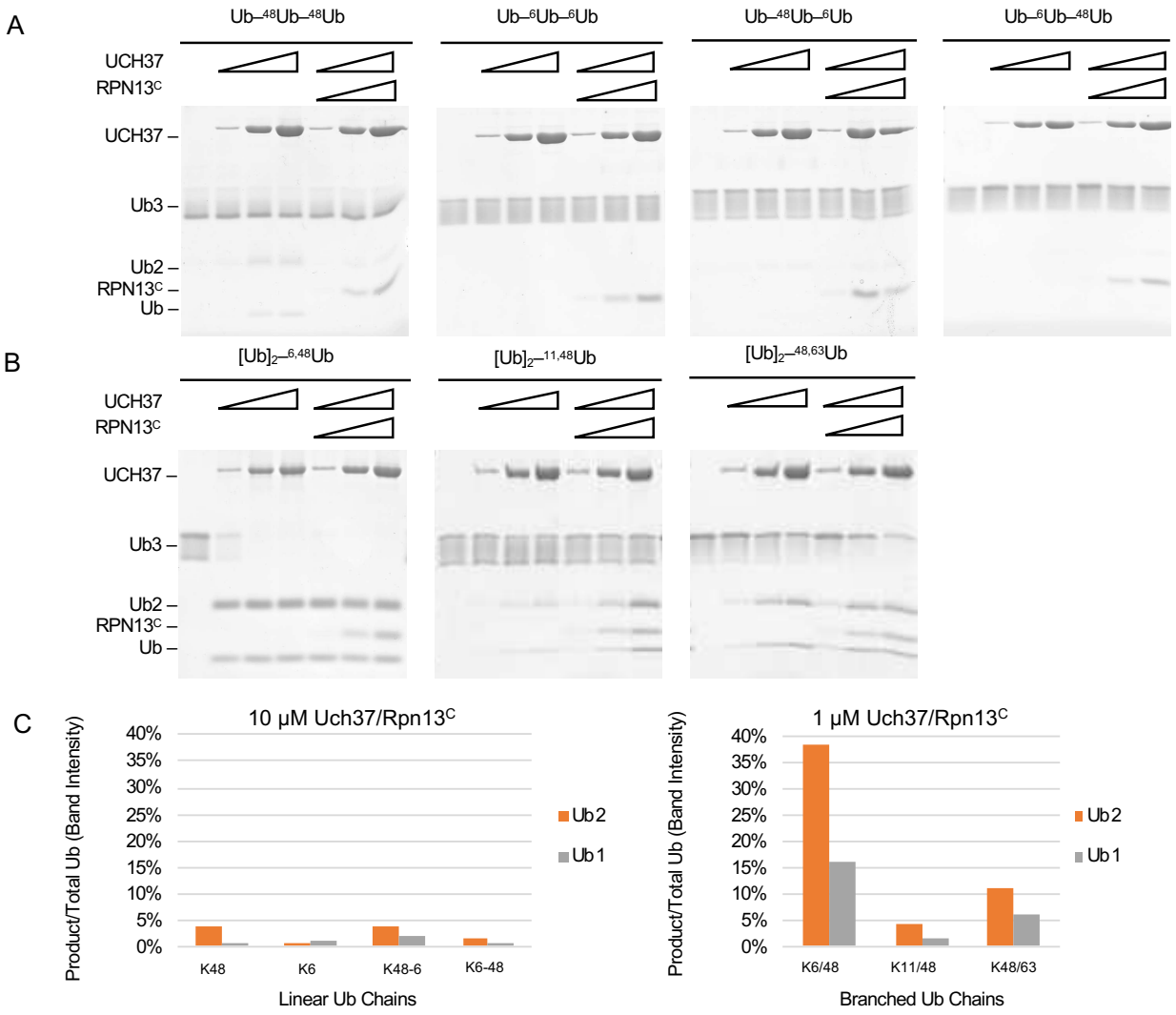

FIG 2.2 UCH37 coordinates with Rpn13^{C} to select for branched Ub chains. (*A*) *In-vitro* UCH37/ RPN13^{C} deubiquitination (DUB) assays analyzed by SDS-PAGE and Coomassie Brilliant Blue stain. 5 μM homotypic or heterotypic linear poly-Ub substrate was incubated with 1, 5, or 10 μM UCH37 alone or with equal molar concentration of RPN13^{C} for 1 hour at 37ºC and quenched with SDS-PAGE running buffer. (*B*) Same as (*A*) but with 5 μM branched Ub chain. *(C)* Quantification of the Ub product bands from Uch37 catalysis relative to total Ub band intensity from the gel-based deubiquitination assays in (*A*) and (*B*). *Left*, quantification of product produced from hydrolysis of 5 μM linear Ub chains by 10 μM UCH37/Rpn13c. *Right,* quantification of product produced from hydrolysis of 5 μM branched Ub chains by 1 μM UCH37/Rpn13c.

against [Ub]$_2$–^{6,48}Ub, western blot against the K6 or K48 linkages led to detection of the Ub–^{6}Ub, but not Ub–^{48}Ub. This revealed that Uch37/Rpn13^{C} exclusively cleaves the K48 linkage (FIG 2.3). To support this further, each DUB assay containing Uch37/Rpn13^{C} with or without the

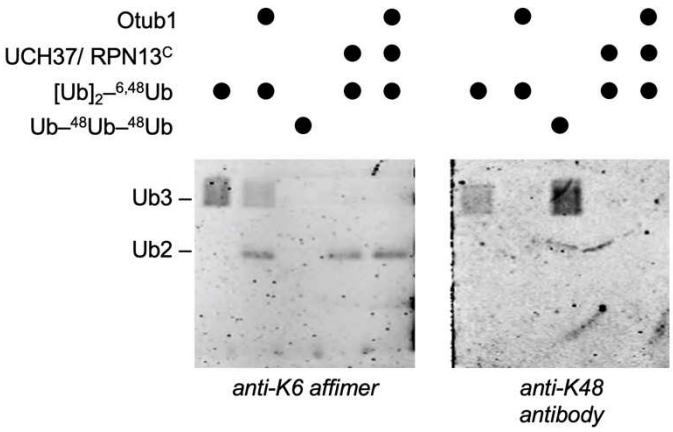

FIG 2.3 Uch37/Rpn13^{C} exclusively cleaves the K48-linkage in K6/K48-linked branched Ub chains. In vitro gel-based DUB assays for linear K48 and branched K6/K48 linked Ub chains were analyzed by western blot. 5 μM Ub chains were incubated with 1 μM of either the K48-specific DUB Otub1 or Uch37/Rpn13c at 37ºC overnight. Left, blot against the K6 linkage using an anti-K6 affimer. Right, blot against the K48 linkage using and anti-K48 antibody.

addition of OTUB1 gave indistinguishable results. Combined with the preference for branched chains, this reveals that Uch37/Rpn13^{C} preferentially cleaves the K48 linkage within K48-linkage containing branched Ub chains.

2.4 Catalysis of branched chains by Uch37 is enhanced by Rpn13, whereas catalysis of linear chains by Uch37 is inhibited by Rpn13.

Association of Uch37 with Rpn13 allows Uch37 to be a functional regulatory component of the 26S proteasome. From the solved crystal structure of Uch37/Rpn13^{C}, the positions of contact between Uch37 and Rpn13^{C} have been identified.[23] Although the primary points of Rpn13^{C} contact are within the Uch37 C-terminal α-helices, three residues of the Uch37 active site crossover loop, R145, M148, and F149, have also been identified as positions of contact by Rpn13^{C}. Rpn13 interaction with Uch37 ASCL holds this otherwise unstructured 21-amino acid loop in a more rigid position projecting away from the Uch37 active site, likely for the purpose of regulating substrate access. Although kinetic studies revealed that Rpn13 increases the rate of Uch37 catalysis of Ub from small adducts (Ub-AMC) relative to Uch37 alone,[23] it is important to

consider how association of Uch37 with Rpn13 affects catalysis toward bulkier, more physiologically relevant poly-Ub substrates.

In vitro Uch37 DUB assays ± Rpn13^{C} incubated with Ub–^{48}Ub–^{48}Ub or [Ub]$_2$–^{6,48}Ub were monitored by SDS-PAGE. The amount of Ub monomer produced was quantified from band intensities and normalized to total Ub in each lane. Results revealed that Rpn13 assists in branched Ub chain substrate selection. In the Uch37 DUB assays containing Ub–^{48}Ub–^{48}Ub, addition of Rpn13^{C} *decreased* catalysis by around 5-fold (Fig. 2.4, B *left*). In DUB assays containing the branched chain [Ub]$_2$–^{6,48}Ub, addition of Rpn13^{C} *increased* catalysis almost 2-fold (Fig. 2.4, B *right*). As the Rpn13 stabilized Uch37 ASCL sterically occludes substrates from the

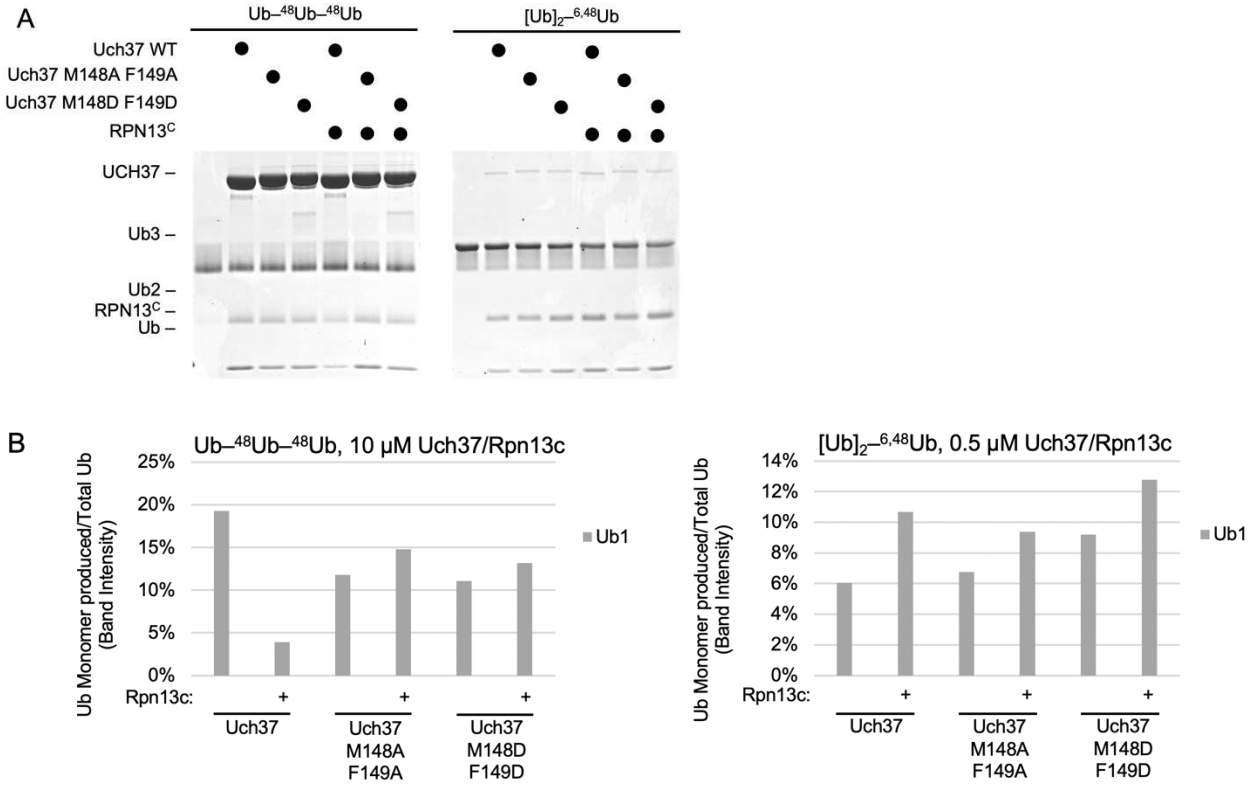

FIG 2.4 Rpn13 stabilizing contacts with Uch37 ASCL enhances substrate selectivity. Comparison of hydrolysis of linear and branched Ub chains with Uch37 WT and ASCL mutants with and without Rpn13^{C}. Left, 10 μM Uch37 ± 10 μM Rpn13^{C} incubated with 5 μM Ub–^{48}Ub–^{48}Ub for 2 hours. Right, 0.5 μM Uch37 ± 0.5 μM Rpn13^{C} incubated with 10 μM [Ub]$_2$–^{6,48}Ub for 2 hours. (B) Differences in either linear or branched chain hydrolysis, with or without Rpn13^{C}, in reactions of WT and Uch37 ASCL mutants monitored by quantification of monoUb band intensity relative to total Ub band intensity.

active site, these results suggest that Rpn13 assists in selecting for and enhancing catalysis of branched Ub chains.

2.5 Rpn13 contacts with Uch37 ASCL at M148 and F149 are important for branched Ub chain specificity

To support the finding that Rpn13 contacts with Uch37 at the ASCL help select for and enhance branched Ub chain catalysis, *in vitro* DUB assays were run with Uch37 containing site specific mutations at two of the three ASCL-Rpn13 contacts. Shown previously, the Uch37 double mutation M148AM149A with Rpn13 showed kinetic parameters for the catalysis of Ub-AMC comparable to that of Uch37 alone.[23] This indicates that this double mutation is sufficient to observe the deleterious effects of disrupting Rpn13 binding to the ASCL.

Using Uch37 M148AF149A, hydrolysis of Ub–^{48}Ub–^{48}Ub or [Ub]$_2$–^{6,48}Ub with or without Rpn13^{C} was monitored to determine how these ASCL contact points affect Uch37 activity toward linear and branched poly-Ub chains. For the linear K48 Ub chain, where WT Uch37/Rpn13 showed significantly reduced catalysis relative to WT Uch37 alone, linear Ub chain catalysis by Uch37 M148AF149A/Rpn13^{C} was close to identical of that for Uch37 alone (Fig. 2.4, B *left*). The same conclusion can be seen when Uch37 ASCL contains M148D and F149D mutations. This suggests that Rpn13 interactions with the Uch37 ASCL through contacts at M148 and F149 help to inhibit Uch37 catalysis toward linear Ub chains.

The same test was run with [Ub]$_2$–^{6,48}Ub. Results revealed that branched Ub chain catalysis, irrespective of WT Uch37 or either Uch37 ASCL mutant, showed increased activity in reactions containing Rpn13 (Fig. 2.4, B *right*). Stated differently, whether or not the ASCL was stabilized at the position of Rpn13 contacts, branched chain catalysis was still enhanced in reactions with Uch37 in complex with Rpn13 relative to those with Uch37 alone. This suggests that the stabilizing contacts of Uch37 ASCL by Rpn13 serve to prevent catalysis of linear Ub chains but not for branched Ub chains. In this way, this interaction provides a gateway-like regulatory mechanism, favoring branched Ub chain substrates over their linear counterparts.

We propose that in the Uch37/Rpn13 complex, containing a stabilized active site crossover loop, the unique topology of the branched Ub chain allows for displacement of this regulatory loop, positioning one of the two Ub–Ub linkage at the active site. Due to the exclusive K48-linkage activity of Uch37 debranching, we propose that some characteristic of the non-K48 Ub in a K48-linkage containing branched Ub chain is responsible for this favorable binding mechanism. Using $[Ub]_2$–^{6,48}Ub as a model, the characteristics of this non K48-linked Ub are probed and discussed in a later section.

2.6 Differences in catalysis are observed between branched Ub substrates containing either C-terminal D77 or di-Gly truncation (ΔGG) at the proximal Ub

Using branched Ub chains containing a C-terminal D77 (a blocking technique to ensure that a particular Ub acts as an acceptor in poly-Ub synthesis) in our free-Ub fluorescent sensor-based kinetics assays (described below), we discovered that Uch37/Rpn13^C cleaves the C-terminal D77 off from the proximal Ub, but with much lower preference than for the K48 linkage (data not shown). The Ub sensor, with high affinity toward the free C-terminus of Ub, bound the proximal Ub of the branched chain after D77 was cleaved, making it difficult to monitor the kinetics of a single catalytic event. We found that the free-Ub sensor does not bind to a ΔGG truncated Ub. The problem was solved when branched chains containing a proximal ΔGG were used in place of those with D77 for measuring catalysis in real time with the free-Ub sensor.

With the results of the sensor-based kinetics assays, there was a notable discrepancy between approximate reaction rates of deubiquitination of the three branched chain types in the kinetics assay (using Ub3(ΔGG)) compared to the gel-based DUB assay (using Ub3(D77)). To test if there is any difference in Uch37/Rpn13^C hydrolysis of branched Ub chains containing C-terminal D77 or ΔGG, gel-based DUB assays were run for each of the three branched Ub chains with either type of proximal Ub C-terminus (FIG 2.5). It was found that Uch37/Rpn13^C consistently cleaves branched Ub chains containing a C-terminal ΔGG faster than those with a C-terminal D77.

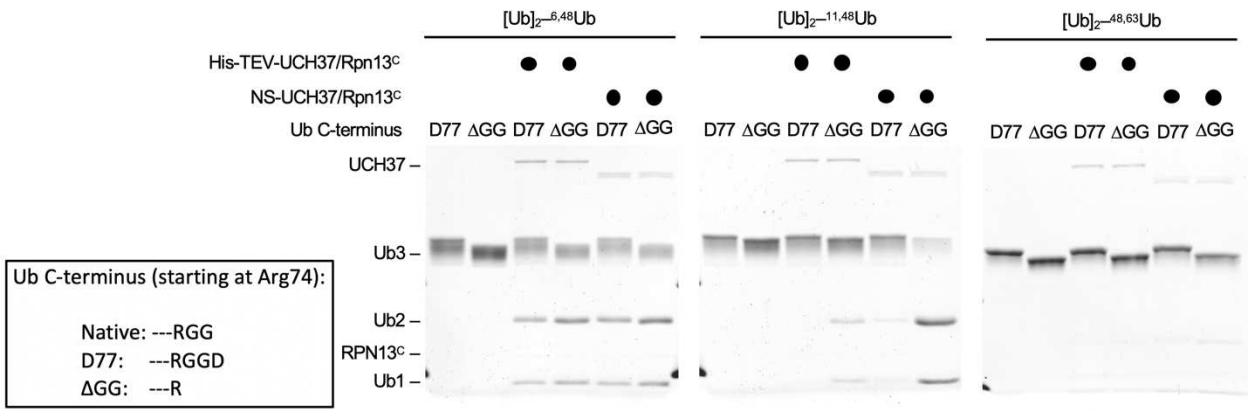

FIG 2.5 Differences in catalysis observed with different Uch37 N-terminal constructs and Ub C-terminal blocking strategies. In vitro DUB assay comparing catalysis of branched chains by NS-Uch37 or His-Uch37 to three types of branched Ub3 substrates containing C-terminal D77 or ΔGG. 1 μM Uch37 was incubated with 5 μM branched Ub chains for 2 hours at 37ºC. Reactions analyzed by SDS-PAGE and Coomassie stain.

Another difference between the gel-based assays and the fluorescent sensor-based kinetics assays was the Uch37 construct used. Previously, the gel-based assays used a His-TEV-6aa-Uch37 (6x His-tag, TEV cleavage site, 6 amino acid linker), whereas the kinetics assays used NS-Uch37 (N-terminal serine in place of methionine, no tag). Each branched chain (containing either D77 or ΔGG) was tested with Uch37/Rpn13^{C} of either Uch37 construct (FIG 2.5). The results revealed that His-TEV-6aa-Uch37/Rpn13^{C} cleaves branched Ub chains (with C-terminal D77) in the order of $[Ub]_2$–^{6,48}Ub, $[Ub]_2$–^{48,63}Ub, $[Ub]_2$–^{11,48}Ub (greatest to least), as observed in the original gel-based assays. NS-Uch37/Rpn13^{C} cleaves branched Ub chains (with C-terminal ΔGG) in the order of $[Ub]_2$–^{11,48}Ub, $[Ub]_2$–^{6,48}Ub, $[Ub]_2$–^{48,63}Ub, as observed in the fluorescent sensor-based kinetics assays. The original assays allowed for the conclusion that branched Ub chains are preferred substrates over linear Ub chains. From here we sought to quantify the differences in hydrolysis between each branched Ub chain. As the kinetics assays use both a Uch37 construct and branched Ub chain more representative of physiological enzyme and substrate, the differences between hydrolysis of each branched chain can be concluded with greater confidence.

2.7 Copurified NS-Uch37/Rpn13^{C} and NS-Uch37/Rpn13^{FL} are no more active than NS-Uch37/Rpn13^{c} from individually purified enzymes

A recent report from the Strieter lab at University of Massachusetts at Amherst suggested that co-purification of Uch37 with Rpn13 as opposed to incubation of each recombinant protein was necessary to observe activity.[32] We co-purified both NS-Uch37/Rpn13^{C} and NS-Uch37/Rpn13^{FL} (full length) and monitored branched chain hydrolysis relative to NS-Uch37/Rpn13^{C} added from individually purified components incubated prior to the start of the reaction. The method of co-purification of NS-Uch37/Rpn13^{C} or NS-Uch37Rpn13^{FL} was followed identically to the method used by Deol K., et al. Our *in vitro* gel-based assay results indicate that there is no increase in activity due to co-purification of the enzyme complex relative to the complex formed from individually purified enzymes (FIG 2.6). These results also confirm past findings that Rpn13^{C} is sufficient to bind and activate Uch37 toward not only Ub-AMC as seen previously, but also branched chains. Comparing the hydrolysis of co-purified NS-Uch37/Rpn13^{C} to co-purified NS-Uch37/Rpn13^{FL}, we must consider the 2-fold greater difference

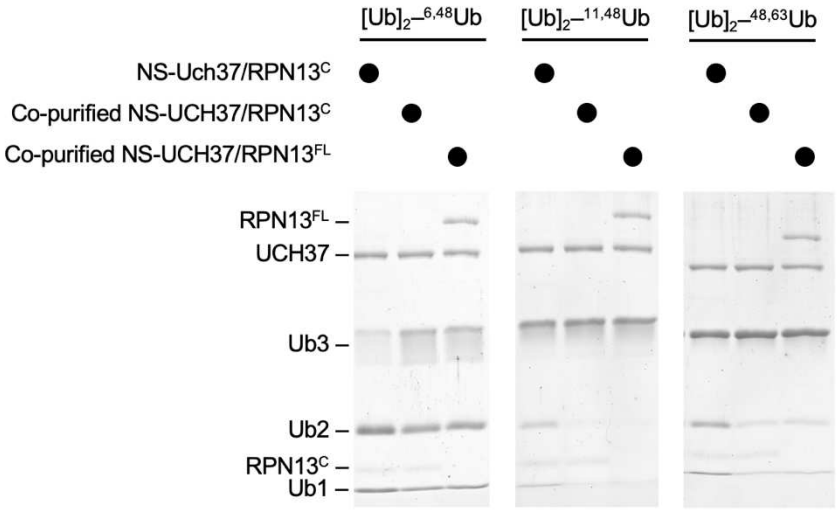

FIG 2.6 Copurified NS-Uch37/Rpn13^{c} and NS-Uch37/Rpn13^{FL} are no more active than NS-Uch37/Rpn13^{c} from individually purified enzymes. *In vitro* DUB assay comparing hydrolysis of branched chains by NS-Uch37 or His-Uch37 to three types of branched Ub3 substrates containing C-terminal D77 or ΔGG. 1 μM Uch37 was incubated with 5 μM branched Ub chains for 2 hours at 37ºC. Reactions analyzed by SDS-PAGE and Coomassie stain.

in baseline activity of the former (Fig 2.1). If the activity of co-purified NS-Uch37/Rpn13^{FL} was multiplied by two to correct for the difference in baseline activity, it can be seen that co-purified NS-Uch37/Rpn13^{FL} activity toward branched Ub chains is slightly greater than co-purified NS-Uch37/Rpn13^{C} and close to the same as NS-Uch37+Rpn13c.

2.8 Discussion

Of important note, Uch37 debranching activity was first discovered by members of the Streiter lab by analyzing Uch37 hydrolyzed branched Ub chains by mass spectrometry as well as gel-based analyses.[32] Our work supports these findings as well as provides novel insights into this enzymatic activity that are discussed throughout this paper.

To our knowledge, Uch37 is the first enzyme identified to have selective activity toward branched Ub chains. As the complexity of the Ub code unfolds and specific functions of branched Ub chains are being determined, the identification of an enzyme that selects for branched Ub chains is an important element in the understanding of Ub signaling. It also opens the possibility that there could be other enzymes or Ub receptors within the cell that operate by recognizing the branched Ub topology. Other UCH family of DUBs, having high degrees of conservation with Uch37, are good candidates for testing potential debranching chain activity. For example, BAP1, a UCH family DUB with tumor suppressing activity, has been proposed to have enzymatic activity similar to UCHL5 (AKA Uch37), although its substrate selection still remains unknown.[33, 34]

It appears that intermolecular contacts between Rpn13 and the Uch37 ASCL assist in Uch37 substrate selection. The 21 amino acid ASCL has a maximum diameter of 20Å, which is too small for Ub to thread through. In order to reach the UCH domain active site, the loop must be displaced in order for a Ub–Ub isopeptide bond to reach the catalytic cysteine. The stabilization of the loop by Rpn13 contacts with Uch37 holds the loop in a conformation projected away from the UCH domain. Our findings suggest that this assists in the selection of branched Ub chains due to their unique three-dimensional structure and ability to

simultaneously displace the loop and reach the active site. The Uch37 ASCL therefore exemplifies a unique mechanism of substrate access/selection.

The results suggesting that Uch37 possesses poly-Ub debranching activity implies that Uch37 plays a unique role in the regulation of branched chain ubiquitinated substrates at the 26S proteasome. Uch37 resides distal to the substrate translocation entry channel. We see that it trims branched Ub chains, an activity that could potentially increase protein turnover by the proteasome. If a substrate is ubiquitinated with a large branching poly-Ub signal, this poly-Ub could allow for faster recognition by the proteasome relative to substrates modified with shorter chains, but equally it could occupy multiple Ub binding sites. We hypothesize that Uch37 could trim branched chains, helping release the Ub from the 19S regulatory particle, allowing for quicker reception of the next proteasome-targeted substrate. Other potential functions of Uch37 debranching at the proteasome could involve enhanced substrate release/rescue similar to Usp14, or possibly Ub chain editing for the purpose of allowing easier *en bloc* deubiquitination by either Usp14 and/or Rpn11. The mechanism of substrate regulation by Uch37 at the proteasome is one that will be addressed in future studies.

2.9 Materials and methods

2.9.1 Plasmids and antibodies

For the expression of Ub, the pET3a-hUb, pET3a-hUb(D77), pET3a-HisUb(G76C) plasmids and variants of Ub in these plasmids generated by mutagenesis were used.[35] For the expression of Uch37, the pET151a 6XHis-TEV-hUch37 plasmid was used.[23] Using the pET151a 6XHis-TEV-hUch37 plasmid as a template, infusion primers were designed and used to both delete the six amino acids that remained on the N-terminus of Uch37 after TEV protease digest and change the N-terminal methionine to a serine. This allowed for the generation of the pET151a NS-Uch37 plasmid. The pDest 15.1 hRpn13(285-407) plasmid was used for the expression of $Rpn13^{C}$.[23] The pET21d 6xHis-hE1 plasmid was used for the expression of the Ub activating enzyme, E1.[36] The pGEX- Cdc34 plasmid was used for the expression of the Ub

conjugating enzyme, Cdc34.[37] The Ub conjugating enzyme UbcH5c was cloned by Yun S. Choi into pET28a plasmid.[38] The pET16b Ubc13 and pET3a MMS2 plasmids were used for the expression of each of respective Ub conjugating enzymes.[39] The pGEX6P1-UBE2S-UBD plasmid was used for the expression of the Ub conjugating enzyme, UBE2S-UBD.[40] The pMCSG170NleL plasmid was used for the expression of the Ub ligating enzyme, NleL.[41]

The following antibodies/affimers were used: The anti di-Ub K6 affimer, purchased from Avacta sciences and rabbit anti-K48 di-Ub monoclonal antibody (Millipore, Cat# 05-1307).

2.9.2 Expression and purification of Ub and Ub conjugating enzymes

Expression and purification of ubiquitin was adapted from Pickart C., et al 2005.[28] The appropriate Ub gene containing plasmid was transformed into Rosetta 2 cells and grown in two liters up to an OD of 0.8-1.0. Cells were induced with 0.4 mM IPTG and grown 4 hrs longer. Harvested cells were lysed with 50 mM Tris-HCl (pH 7.6), 1X protease inhibitor cocktail, and 0.4 mg/ml lysozyme. If the Ub contained a cysteine residue, 1 mM DTT was added to the buffer. DNA was digested by the addition of 10 mM $MgCl_2$, and 20 ug/ml DNase I. The solution was centrifuged at 8000 rpm for 20 minutes and the soluble fraction was collected. Cellular protein was precipitated by the addition of 70% perchloric acid to a final concentration of 0.5%. The solution was centrifuged as before and the soluble fraction containing ubiquitin was collected. The perchloric acid containing solution was dialyzed twice for 4 hours or longer against 50 mM ammonium acetate, pH 4.5, 1 mM EDTA, and 1 mM DTT. The acidified Ub containing solution was then purified over cation exchange chromatography using a buffer of 50 mM ammonium acetate and a gradient of 0-0.5 M NaCl. The fractions containing Ub were pooled, concentrated using Amicon Ultra-15 Centrifugal Filters, and the pH was adjusted to 7.5 using Tris base.

The Ub activating enzyme E1 was purified from the pET21d 6xHis-hE1 plasmid according to the methods established in Berndsen C.E., et al. 2011, by Aixin Song.[36] The pET28a UbcH5c plasmid was expressed and purified by Yun S. Choi according to established methods in Choi Y.S., et al, 2019.[38] 10xHis-Mms2 and Ubc13 Ub conjugating enzymes were

expressed and purified by Yun S. Choi from the pET16b and pET31 plasmids, respectively, according to Hofmann R.M., et al., 1999.[39] The Ub conjugating enzyme UBE2S-UBD was purified from the pGEX6P1-UBE2S-UBD plasmid by Benjamin Shmidt according to methods from Bremm A., et al., 2010.[40] The pGEX-GST-Cdc34 plasmid was transformed into BL21(DE3) CodonPlus cells, grown and expressed in 2xYT media. At an OD = 0.6, expression was induced with 0.4 mM IPTG and grown 4 hrs longer, till the cells were harvested. Cell pellets were resuspended in lysis buffer (50 mM Tris pH 8, 1% Triton X-100, 0.5 M NaCl, 10 mM EDTA, 10 mM EGTA, 10% glycerol, 5 mM DTT, 0.1 mM PMSF, 5 µg/ml Antipain, and 1 µg/ml Leupeptin), lysed by sonication, and centrifuged. The soluble fraction was mixed with glutathione-S-Sepharose beads equilibrated in lysis buffer and incubated at 4ºC for 2 hours. Buffer was drained and equilibrated in thrombin cleavage buffer (25 mM Tris pH 7.6, 0.1 M NaCl, 5 mM DTT, and 1 mM EDTA). 150 µl of 1 U/µl Thrombin was added to the protein bound column solution and incubated at 2.5 hours at 22ºC to cleave Cdc34 from the column. Eluted protein was purified further over anion exchange chromatography using a Mono Q column and a gradient of cleavage buffer from 0 – 1.0 M NaCl. Fractions containing purified Cdc34 were pooled, concentrated, and frozen for storage at -80ºC. The E3, NleL was expressed and purified according to Lin D., et al., 2007, by Aixin Song.[41]

2.9.3 Synthesis and purification of poly-Ub chains with different topologies

Polyubiquitin chains of defined linkages and topologies were synthesized according to the methods established in Pickart C., 2005. Ub was expressed and purified as described above blocked either at the C-terminal position or at specific lysine residues to block conjugation. C-terminally blocked Ub was generated by expressing Ub with either an additional aspartic acid (Ub(D77)) or a truncation of the C-terminal diGly (ΔGG). Lysine residues were mutated to arginine by site-specific mutagenesis to prevent further conjugation at those positions.

Branched Ub chains were synthesized in ubiquitination buffer (50 mM Tris, pH 7.6, 50 mM NaCl, 0.5 mM EDTA, and 5 mM MgCl2) in one of two ways. For the $[Ub]_2$-^{6,48}Ub branched

chain, distally blocked Ub (K-to-R mutations at desired linkage positions) were combined with proximally blocked Ub in a 2:1 molar ratio with E1, the Ub conjugation enzyme UbcH5c and the Ub ligating enzyme NleL to direct the 6,48 linkages. For the $[Ub]_2$-^{11,48}Ub and the $[Ub]_2$-^{48,63}Ub branched chains, the individual K11 or K63 dimers were generated first using E1/UBE2S and E1/UBC13/MMS2, respectively, each containing a K48R mutation on the distal Ub. The K48 linkage was then directed using E1 and Cdc34.

Linear chains were synthesized in a stepwise fashion by first generating the desired Ub dimer. For the purpose of trimer synthesis, the C-terminus was deblocked by cleavage of the C-terminal D77 with the DUB YUH1. Deblocking reactions took place by incubation at 37ºC for 1 hour in 50 mM Tris-HCl (pH7.6), 1 mM EDTA, 1 mM fresh DTT, and 0.14 mg/ml YUH1. YUH1 was removed by passage through Q Sepharose Fast Flow resin pre-equilibrated with Q buffer (50 mM Tris-HCl (pH7.6), 1 mM EDTA, 5 mM DTT) for 1 hour at 25ºC. Unbound fractions were collected with four washes and concentrated using Amicon Ultra 15 ml Centrifugal Filters. The deblocked dimer was then used in subsequent Ub conjugation assays to generate either linear homo- or heterotypic Ub trimers.

After synthesis, all native chain reactions were acidified using 1/5 volume of 2N Acetic Acid, then purified using Mono S cation exchange chromatography with buffer A (50 mM ammonium acetate) and eluted across a gradient of buffer B (Buffer A + 1M NaCl). Purified fractions were pooled and concentrated by centrifugation in Amicon Ultra-15 Centrifugal Filters up to 10 mg/ml, pH was increased with Tris base to pH 7.5, and samples were stored at -80ºC.

2.9.4 Expression and co-purification of Uch37/Rpn13^{C}

His-Uch37 and GST-Rpn13 were expressed and purified as described previously.[23] His-Uch37 WT and M148F149 mutants were gifts from Benjamin Schmidt. pET151a 6XHis-TEV-hUch37 or pDest 15.1 hRpn13(285-407) were transformed separately in BL21(DE3) CodonPlus cells and expressed in ZYP-5052 autoinduction media.[42] Cells were grown to an OD of around

1.0 then transferred to 19ºC for 20 hrs. Cells were harvested, and pellets were frozen at -80ºC until ready for purification.

Uch37/Rpn13^{C} complex was co-purified as described previously (VanderLinden R.T., et al, 2015). Individual proteins were expressed as described above. For complex co-purification, expression of each protein was monitored by SDS-PAGE and pellets were combined in an approximate 1:1 ratio of each protein. Cells were resuspended in lysis buffer (20 mM Tris-HCl (pH 7.5), 300 mM NaCl, 10 mM imidazole, 0.5% Triton X-100, and the protease inhibitors leupeptin, pepstatin, aprotinin, and PMSF) and sonicated. Lysate was clarified by centrifugation and incubated with Ni-NTA resin pre-equilibrated with lysis buffer for 1 hour. Resin was washed with 6 CV of lysis buffer prior to elution with lysis buffer containing 250 mM imidazole. The eluted protein was then incubated with glutathione agarose resin pre-incubated in GST Binding Buffer (25 mM Tris, pH 7.6, 50 mM NaCl, 1 mM DTT, and 1 mM EDTA). Protein solution was mixed for 1 hour at 25ºC, then washed with 10 CV with GST binding buffer. Resin was brought to a 50% slurry, TEV protease was added in a ration of 1:40 TEV to total protein and incubated at 4ºC overnight. Eluted TEV cleaved complex was collected and the resin was washed with 3CV of GST binding buffer. Complex containing eluate was then pooled and incubated a second time in Ni-NTA resin pre-equilibrated with the original lysis buffer. After incubation for 1 hr at 4ºC, the flow through was collected and the resin was washed with 6 CV of lysis buffer. Samples containing complex were then purified using Mono Q chromatography using buffer A (25 mM Tris, pH 7.6, 10 mM imidazole, and 1 mM DTT), eluted across a gradient of buffer B (Buffer A + 1M NaCl). Samples containing purified complex were pooled after the Q column. If needed, a final size exclusion step using a Superdex 200 column was used to purify the enzyme complex further. Samples were purified in this final step using 50 mM HEPES pH 7.5, 50 mM NaCl, 1mM EDTA, and 1 mM TCEP.

For the purification of His-Uch37 alone, the Ni-resin bound protein was cleaved off with TEV protease and the eluate was run over a Mono Q column and a Superdex 200 column. For

the purification of $Rpn13^{C}$ alone, the protein was purified by a series of GST resin affinity column, Mono Q column, and Superdex 200 column purification steps similarly as described above.

2.9.5 In vitro gel-based deubiquitination assays

Individually expressed and purified recombinant Uch37 and Rpn13 ($Rpn13^{C}$ or $Rpn13^{FL}$) were added together in equimolar concentrations and incubated at 25ºC for 30 minutes. 0.5 μM, 1 μM, 5 μM, or 10 μM Uch37/Rpn13(C or FL) was added to 50 mM HEPES (pH 7.5), 50 mM NaCl, 2 mM DTT. The reaction was initiated by the addition of 5 μM polyubiquitin substrate. Reactions were incubated at 37ºC, samples were taken at defined time points and quenched with SDS-PAGE running buffer. Samples were analyzed via SDS-PAGE on 13.5% gels followed by either Coomassie Brilliant Blue staining or subject to western blot analysis. Where indicated, gels were quantified using ImageQuant TL image analysis software.

CHAPTER 3: THE KINETICS OF UCH37/$RPN13^{C}$ DEBRANCHING

3.1 Introduction

After the identification of Uch37/Rpn13 substrate specificity and a number of characteristics regarding its mechanism of catalysis, we sought to characterize the kinetic parameters of this enzyme-substrate reaction. We began by determining if differences in substrate selection are achieved by differences in enzyme/substrate binding affinities. Using a His-tagged catalytically inactive Uch37 active site mutant (His-Uch37(C88S)) in complex with $Rpn13^{C}$, RED-tris-NTA (a fluorophore specific for labeling his-tagged molecules), a fluorescence based technique called microscale thermophoresis (MST), and a Monolith NT.115 instrument (NanoTemper Technologies), we were able to measure the dissociation constant, K_D, for a wide variety of poly-Ub chains. MST is a method that allows for the calculation of K_D values by measuring the thermophoresis (or movement toward or away from a local IR induced heat stimulus) of fluorophore labelled enzyme in binding equilibrium with unlabeled Ub chain.

Fluorescence is measured as a function of time pre- and post-infrared laser stimulation. Thermophoresis is measured as the magnitude of difference in fluorescence between pre-IR and 5-seconds post-IR stimulation. Thermophoresis is measured for a series of binding reactions at titrating substrate concentrations. Plotting thermophoresis as a function of substrate concentration then allows for the calculation of the dissociation constant K_D.

Once binding affinities of Uch37/Rpn13^C were established, we set out to determine the Michaelis-Menten kinetic parameters of debranching. Using an Atto532-tUI free-Ub sensor, with sub-nanomolar affinity toward free Ub,[38] we were able to monitor the kinetics of Uch37/Rpn13^C branched chain deubiquitination in real time. Using branched Ub chains with C-terminal ΔGG truncation on the proximal Ub (a position that is not bound by Atto532-tUI), cleavage of the K48 linkage releases a single Ub. Upon binding of this free Ub C-terminus by the Atto532-tUI, fluorescence increases (FIG 3.2, A). The increase in fluorescence due to debranching was monitored over time using a FluoroMax-4 spectrofluorometer (HORIBA Scientific) for a series of enzyme reactions with varying substrate concentrations. From the initial linear portion of each progression curve, the initial rate of reaction (V_0) was calculated. V_0 was plotted against substrate concentration to give the Michaelis-Menten kinetics curve for hydrolysis of each type of branched chain. Using GraphPad Prism, K_M and V_{max} values were determined from each kinetics curve. k_{cat} values were calculated by dividing V_{max} by the enzyme concentration in each reaction. The Michaelis-Menten analysis of Uch37/Rpn13^C allowed for the determination of the maximum rate of catalysis per enzyme, k_{cat}, and the substrate concentration at ½ V_{max}, K_M. This information revealed the differences in the hydrolysis of each branched chain type and provided information on the speed of Uch37 enzymatic activity. Using these two approaches, we were able to quantify Uch37/Rpn13^C activity, observe differences in hydrolysis between different poly-Ub substrates, and predict how this catalytic activity might affect the function of Uch37/Rpn13^C at the proteasome.

A

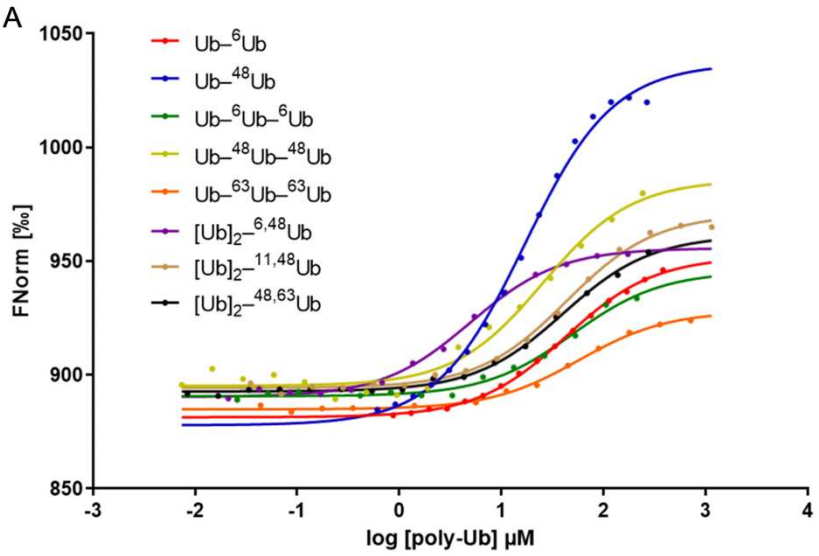

B

		Ub C-terminus	K_D (µM)
Linear	**Ub–^{6}Ub**	**D77**	42.1 ± 0.6
	Ub–^{48}Ub	**ΔGG**	16.8 ± 2.5
	Ub–^{6}Ub–^{6}Ub	**D77**	50.0 ± 3.5
	Ub–^{48}Ub–^{48}Ub	**GG**	25.4 ± 5.5
	Ub–^{63}Ub–^{63}Ub	**GG**	56.9 ± 1.0
Branched	**[Ub]$_2$–^{6,48}Ub**	**D77**	4.9 ± 1.0
	[Ub]$_2$–^{11,48}Ub	**D77**	43.4 ± 1.3
	[Ub]$_2$–^{48,63}Ub	**D77**	40.1 ± 1.6

FIG 3.1 Uch37/Rpn13^{C} has the highest affinity for K6/K48-linked branched Ub chains. (A) Binding curves for RED-tris-NTA labelled His-Uch37(C88S)/Rpn13^{C} toward linear homotypic Ub chains, linear heterotypic Ub chains and branched Ub chains. For each Ub chain type, normalized fluorescence (FNorm)was determined by monitoring the thermophoresis between 0 and 5 seconds at each of 16 poly-Ub substrate concentrations in binding equilibrium with 50 nM Uch37(C88S)/Rpn13^{C}. FNorm was plotted against the log [Ub] (µM) for each Ub chain type to determine the binding affinity of Uch37/Rpn13^{C} toward each poly-Ub type. (B) Binding affinity (K_D) values determined from the curves shown in (A) by fitting with the equation Y = Bottom + (Top-Bottom)/(1+10^(LogEC$_{50}$-X)), where Bottom and Top are plateaus in units of per mille and EC$_{50}$ (treated here as the K_D) is the concentration of poly-Ub that gives a response halfway between Bottom and Top. K_D values are reported ± standard error (SE) in µM.

3.2 Uch37(C88S)/Rpn13^{C} has the highest binding affinity toward the [Ub]$_2$–^{6,48}Ub branched chain

Using microscale thermophoresis, the measurement of the K_D values for His-Uch37(C88S)/Rpn13^{C} toward linear and branched poly-Ub chains revealed that Uch37/Rpn13^{C} has the highest binding affinity, or lowest K_D value, for the [Ub]$_2$–^{6,48}Ub branched chain at 4.9 ± 1.0 μM (FIG 3.1). Homotypic K48 linked chains showed the next highest binding affinity at 16.8 ± 2.5 μM and 25.4 ± 5.5 μM for Ub–^{48}Ub and Ub–^{48}Ub–^{48}Ub, respectively. Due to the small difference between K48-linked Ub2 and Ub3, we conclude that an extra K48 linkage does not increase binding affinity toward Uch37/Rpn13^{C}. This is consistent with the K_D values determined for Ub–^{6}Ub and Ub–^{6}Ub–^{6}Ub at 42.1 ± 0.6 μM and 50 ± 3.5 μM, respectively. K_D values for the other two branched Ub chains measured are similar to the linear Ub trimers. However, as observed in the gel-based DUB assays, hydrolysis is primarily observed for branched Ub chain substrates. Therefore, despite similar affinities for some branched and linear chains, a branched chain is necessary for Uch37 deubiquitination. As noted in Fig 3.1, B, two linear Ub chains posessed a free C-terminus (GG) and one posessed the C-terminal truncation (ΔGG). It is possible that K_D values are affected by the slight changes in the poly-Ub chain C-terminus, which will need to be addressed in the future.

3.3 Uch37/Rpn13^{C} Michaelis-Menten kinetics analysis

Fluorescence-based Michaelis-Menten kinetics analysis revealed that Uch37/Rpn13^{C} has the lowest K_M value for the [Ub]$_2$–^{6,48}Ub, followed by [Ub]$_2$–^{11,48}Ub, and [Ub]$_2$–^{48,63}Ub (FIG 3.2, B). This means that Uch37/Rpn13^{C} can reach V_{max} at lower concentrations of [Ub]$_2$–^{6,48}Ub compared to the other branched Ub chains tested. As K_M values are, in part, a representation of enzyme-substrate affinity, the K_M values determined in this analysis are consistent with our K_D values determined from the MST analysis.

Our kinetics assay revealed that under saturating substrate concentrations, Uch37/Rpn13^{C} hydrolyzes branched Ub chains at around 0.4 - 3.2 min^{-1}, with the slowest

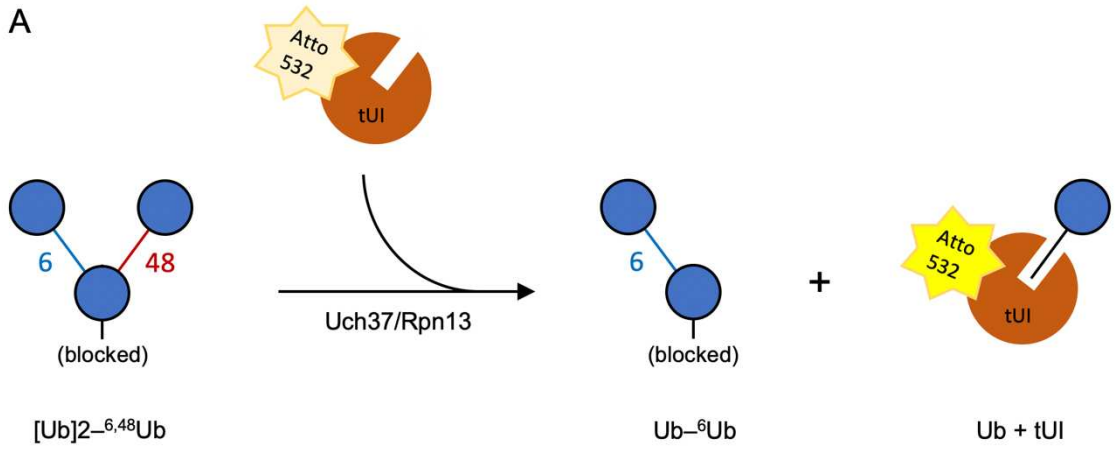

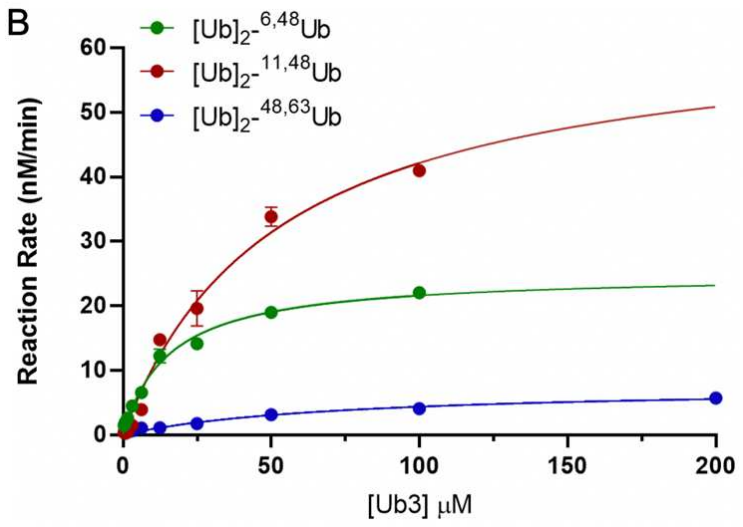

	K_M (μM)	k_{cat} (min^{-1})	k_{cat}/K_M ($min^{-1}μM^{-1}$)
$[Ub]_2$–^{6,48}Ub	16 ± 1.5	1.25 ± 0.04	0.08 ± 0.03
$[Ub]_2$–^{11,48}Ub	52 ± 8.8	3.2 ± 0.3	0.06 ± 0.03
$[Ub]_2$–^{48,63}Ub	75 ± 14	0.38 ± 0.03	0.005 ± 0.002

FIG 3.2 (*A*) Illustration for monitoring branched chain deubiquitination in real time using an Atto532-tUI free Ub sensor. Uch37 cleaves branched chains at the K48 linkage, and free Ub is released. This Ub is bound by Atto-532-tUI and upon binding, Atto532 fluorescence increases. (*B*) Real-time kinetic analysis of UCH37/RPN13^C deubiquitination of branched Ub chains. Fluorescence increase due to NS-Uch37/Rpn13^C branched chain deubiquitination and Atto532-tUI binding to free Ub was monitored over time using a FluoroMax-4 fluorometer (HORIBA Scientific). Initial velocity (V_0) was determined for nine reactions across different branched chain substrate concentrations and was plotted against substrate concentration. Curves were fit using GraphPad Prism to determine K_M and k_{cat} for Uch37 catalysis of each substrate. Each reaction was run in duplicate. Error bars indicate the SE of duplicate values. K_M, k_{cat}, and k_{cat}/K_M values are reported ± SE.

catalysis for the $[Ub]_2$–^{48,63}Ub and the fastest for $[Ub]_2$–^{11,48}Ub (FIG 3.2, B). These values reveal the speed of catalysis of a single Uch37/Rpn13^C enzyme complex at saturating substrate concentrations. These k_{cat} values show again that the $[Ub]_2$–^{48,63}Ub branched chain is a less favorable substrate relative to the other substrates measured. These k_{cat} values also provide values to compare the rates of enzyme catalysis to other DUBs.

Dividing the k_{cat} value by K_M gives a value for the catalytic efficiency of Uch37/Rpn13^C debranching for each branched Ub chain type. With k_{cat}/K_M values of $[Ub]_2$–^{6,48}Ub roughly equivalent for that of $[Ub]_2$–^{11,48}Ub, we can see that both of these branched Ub chains are equally preferred substrates for hydrolysis by Uch37/Rpn13^C (FIG 3.2, B). With a 10-fold lower k_{cat}/K_M value for $[Ub]_2$–^{48,63}Ub, we can conclude that this is a less preferred branched chain substrate for Uch37/Rpn13c.

3.4 Discussion

Binding affinity analysis between Uch37/Rpn13^C and the various poly-Ub substrates reveals that the branched Ub chain linked at K6 and K48 is a favored substrate. The gel-based analyses revealing the highest substrate preference of Uch37/Rpn13^C for $[Ub]_2$–^{6,48}Ub can be explained in part, by the finding that Uch37/Rpn13^C has the highest binding affinity for the $[Ub]_2$–^{6,48}Ub by about 8-fold over other branched chain substrates. Despite the relatively high binding affinities for Ub–^{48}Ub and Ub–^{48}Ub–^{48}Ub, a K48 linkage combined with another branched linkage does not always make for a tightly bound substrate. Both $[Ub]_2$–^{11,48}Ub and $[Ub]_2$–^{48,63}Ub branched trimers have 8 to 9-fold lower binding affinity than the $[Ub]_2$–^{6,48}Ub branched trimer. Interestingly, despite the differences in binding affinity seen between branched Ub chains and linear Ub chains, Uch37/Rpn13^C substrate hydrolysis largely only occurs for substrates containing the branched topology. Therefore, the substrate topology and its ability to bind Uch37/Rpn13^C in such a way as to displace the ASCL and reach the active site seems to be of greater importance than the affinity of the binding interaction.

Similar work reported from the Strieter lab has led to the determination of K_D values for a number of K48 linear Ub chains and K6/K48 containing branched Ub chains.[32] Their pre-published results revealed Uch37/Rpn13 binding affinity about 10-fold tighter than those reported here. The differences in methodologies include their use of a C88A mutant of Uch37 as opposed to our use of Uch37(C88S) as well as their use of ITC as a means of determining binding affinities. One study has revealed that active site alanine mutations have the potential for enhancing binding of a DUB toward Ub which could explain some of the observed differences.[43] A major difference reported from the Strieter lab was that the K48 linkage provided the high binding affinity toward Uch37 independent of the branched chain topology. Further studies will be necessary to resolve these observed discrepancies.

The Michaelis-Menten kinetics analysis of Uch37/Rpn13^C branched chain hydrolysis revealed differences in the catalysis between the types of branched Ub chains. Where the binding affinity analysis revealed that Uch37/Rpn13^C has the highest binding affinity toward the $[Ub]_2$–^{6,48}Ub branched chain, the sensor-based kinetics assay revealed that Uch37/Rpn13^C has the fastest rate of hydrolysis for the $[Ub]_2$–^{11,48}Ub branched chain. Hydrolysis of the $[Ub]_2$–^{11,48}Ub branched chain being the fastest among the three tested proves that this branched chain type is also a favorable substrate. This analysis also reveals that not all branched chains are suitable substrates for Uch37/Rpn13^C. Both the binding and kinetics analysis of Uch37/Rpn13^C toward the $[Ub]_2$–^{48,63} Ub reveal the lowest binding affinity, the highest K_M, and the slowest rate of catalysis. Therefore, not only is a branched chain needed for catalysis by Uch37/Rpn13^C, but the position of each Ub within the branched chain is important for selection by Uch37/Rpn13^C. Both of the kinetics analyses and previous results from the gel-based assays (FIG 2.2, A), identify two specific branched Ub chain types as favorable substrates for Uch37/Rpn13^C, those being branched Ub chains linked at K6/K48 and K11/K48. Notably, Michaelis-Menten analysis from Deol K.K., et al revealed around a 7-fold higher k_{cat} value for the hydrolysis of $[Ub]_2$–^{6,48}Ub by Uch37/Rpn13^C. Differences could potentially be due to the different methods used for each

kinetic analysis as they monitored deubiquitination over time via SDS-PAGE. Regardless of the difference in k_{cat} values determined, we are still able to conclude that the $[Ub]_2$–^{6,48}Ub branched chain is a favorable substrate for Uch37 hydrolysis.

Our kinetics analysis also revealed that hydrolysis of branched chains by Uch37/Rpn13^{C} is on the order of 1.0 – 3.0 min^{-1}, or one catalytic event every 20 – 60 seconds. Kinetics analyses of proteasomal degradation of a ubiquitinated titin-I27 model substrate showed complete degradation to occur from 20 – 50 seconds, depending on the degree of substrate ubiquitination and the intrinsic stability of the protein.[44] Given that degradation occurs faster than debranching, it is possible that debranching could be too slow to make a difference in the fate of a ubiquitinated proteasome-targeted protein. It is also possible that the activity of Uch37 at the proteasome is important for releasing Ub chains even after they might have been removed *en bloc* from the substrate. As our analyses use poly-Ub substrates and free Uch37/Rpn13^{C}, it is unknown whether or not the efficiency of the Ub chain hydrolysis will increase once Uch37 is bound to the proteasome. Future studies (discussed later) will analyze the differences in proteasome-mediated degradation of proteins modified with branched or linear Ub chains and with Uch37 bound or Uch37 null proteasomes.

3.5 Materials and Methods

3.5.1 Microscale thermophoresis assay to determine enzyme-substrate binding affinity

His-Uch37(C88S)/Rpn13^{C} was labelled with a Red-tris-NTA fluorophore by adding each in 1X Phosphate Buffered Saline with 0.05% Tween 20 (PBST) to 100 nM and 50 nM respectively. K48 and K63-linked Ub3 are gifts from Dr. Robert Cohen. After Ub substrate was 1.5-fold serial diluted over 16 reactions in 1X PBST, the fluorophore labelled enzyme complex was added to a final concentration of 25 nM labelled complex. Each of the 16 reactions were loaded in Monolith NT.115 Standard Treated Glass Capillaries. Each capillary was loaded into capillary trays and placed in the Monolith NT.115 instrument. Thermophoresis was measured across IR stimulation of each sample. Normalized fluorescence, F_{norm}, is determined by dividing

the fluorescence value five seconds after IR laser stimulation (F_1) by the fluorescence value before laser stimulation (F_0). F_{norm} was plotted against substrate concentration to determine the binding affinity (K_D). According to nanotempertech.com /nanopedia/kd-fit-model/, binding curves were fitted with an equation similar to one for the sum of the least squares (x^2), but that allows for less of an influence on the fit from biological outliers. This equation is $\rho(z) = 2(\text{sqrt}(1+z) - 1)$, where $z = x^2$.

3.5.2 tUI-Atto532 sensor-based Michaelis-Menten-kinetics Deubiquitination assay

The kinetics of Uch37/Rpn13^C activity was determined by monitoring deubiquitination in real time with Atto532-tUI, a free Ub sensor designed, expressed and labeled by Yun Choi.[38] A standard curve of fluorescence versus Ub bound sensor was generated by monitoring the fluorescence of solutions of 500 nM Ub sensor with a series of 4 Ub concentrations 3-fold serial diluted from 1.2 μM and one without Ub. The first solution of 1.2 μM determined the fluorescence from saturating bound sensor, where the proceeding solutions established the standard curve. For the kinetics assays, branched chain Ub substrate was serial diluted in 50 mM HEPES (pH 7.5), 5 mM DTT, 50 mM NaCl, and 0.2 mg/ml ovalbumin. Ub sensor was added to 500 nM and reactions were started by adding pre-incubated Uch37/Rpn13^C complex to a final concentration of 20 nM or 40 nM. Branched chain hydrolysis was monitored over 500 seconds using a FluoroMax-4 fluorimeter (HORIBA Scientific) with excitation at 532 nm (slit width 4 nm) and emission at 553 nm (slit width 3 nm). Fluorescence increase was plotted over time, and Δfluorescence/Δtime was determined for each reaction using the linear portion of each reaction curve. V_0 was calculated by comparing Δfluorescence/Δtime with a standard curve to calculate Δ[substrate]/Δtime. In GraphPad prism, V_0 was plotted for each substrate concentration, and modeled as a nonlinear regression Michaelis-Menten analysis. From the each curve fit K_M was determined as the substrate concentration at ½ V_{max}, V_{max} values were determined as V_0 at saturating substrate concentrations, and kcat was measured by dividing V_{max} by the enzyme concentration. All reactions were run in duplicate.

CHAPTER 4: STRUCTURAL FEATURES OF THE SUBSTRATE REQUIRED FOR DEBRANCHING BY UCH37

4.1 Introduction

In vitro analysis of Uch37/Rpn13^{C} activity has provided evidence suggesting that this UCH family DUB enzyme bound to the proteasome subunit Rpn13 selectively catalyzes the deubiquitination of Ub chains containing a branch. Our data suggests that binding of Uch37 to Rpn13 increases selectivity for branched Ub chains in part by stabilizing contacts of the Uch37 ASCL with Rpn13. This generates a "selective substrate gateway," where access to the active site requires displacement of the ASCL. The question remains as to what structural features of both enzyme and substrate are necessary for recognition and hydrolysis of branched Ub chains. Using $[Ub]_2$–^{6,48}Ub as a model, we observed that hydrolysis occurs exclusively at the K48 linkage. We also see that the hydrolysis of mixed linkage linear Ub–^{48}Ub–^{6}Ub and Ub–^{6}Ub–^{48}Ub is negligeable compared to that of the branched $[Ub]_2$–^{6,48}Ub. We propose, therefore, that some characteristic of the K6-linked Ub (or more generally the non K48-linked Ub) in a K48 containing branched chain is necessary for catalysis. The K6 Ub in the branched Ub chain potentially functions to either displace the ASCL directly, or its binding to Uch37 leads to the direct or indirect displacement of the ASCL. Using the $[Ub]_2$–^{6,48}Ub branched Ub chain, we probed the characteristics of the K6-linked Ub needed for successful catalysis by Uch37/Rpn13^{C}.

In order to probe the proposed functions of the K6-linked Ub in the $[Ub]_2$–^{6,48}Ub branched Ub chain, we planned to synthesize K6/K48-linked branched Ub chains with site specific mutations to the K6-linked Ub or a replacement of the K6-linked Ub with a Ub like molecule. If the Ub at this position serves to displace the ASCL independent of any specific binding interaction with Uch37/Rpn13, then replacing the Ub linked to the K6 position with a Ub-like molecule would produce a branched chain equally suitable for recognition and catalysis by Uch37. If a specific binding interface between the K6-linked Ub and Uch37/Rpn13 is required for branched chain substrate selection, then mutations of surface interfaces that participate in this

interaction at either the K6-linked Ub or the enzymes would allow for probing of this question. The second approach requires that specific locations on either Ub or Uch37 be proposed as important locations for this binding interaction. A number of unique positions have been identified on Ub that function in binding to enzymes or Ub binding domains.[45] Of the various Ub surface positions, the Ub hydrophobic patch composed of L8, I44, and V70 serves as an important location for the binding and activation by E1, the Ub activating enzyme.[46] In the context of poly-Ub chains, the Ub hydrophobic patch is also important for efficient targeting of a ubiquitinated substrate to the proteasome.[47] Given the importance of this Ub surface in the recognition and binding by a variety of effectors, we chose this position to first probe the interaction between the branched chain K6-linked Ub and Uch37/Rpn13^{C}.

4.2 An improved Ub–Ub linkage mimic generated by Ub_{75}-mercaptoethylamide (Ub_{75}-MEA) and dichloroacetone (DCA)

One challenge to generating branched Ub chains containing variations of Ub linked at the K6 position is that currently there are no known Ub conjugating enzymes that can generate K6 linkages between Ub and Ub-like molecules or between Ub and a hydrophobic patch mutant of Ub. To solve this problem, we adopted an approach utilizing the chemistry of crosslinking between two cysteine thiols and the small chemical dichloroacetone (DCA).[48] To determine if a K6/K48-linked branched Ub chain crosslinked at the K6 position is a suitable mimic of the native linked $[Ub]_2$–^{6,48}Ub, Uch37/Rpn13^{C} deubiquitination of crosslinked mimic branched chains was compared to native-linkage branched chains and analyzed as before by SDS-PAGE and Coomassie stain.

The first approach to generate a suitable crosslinked $[Ub]_2$–^{6,48}Ub branched chain was to crosslink the cysteine of Ub G76C to the cysteine of a proximal Ub K6C of a K48-linked Ub2 (Mimic 1: K6*/K48). Comparing this crosslinked bond to the native isopeptide bond shows a high degree of similarity, aside from an additional C–C bond length (~1.5 Å) and additional carboxylic acid functional group from the distal Ub C-terminus (Fig. 4.1, A; distal Ub (red),

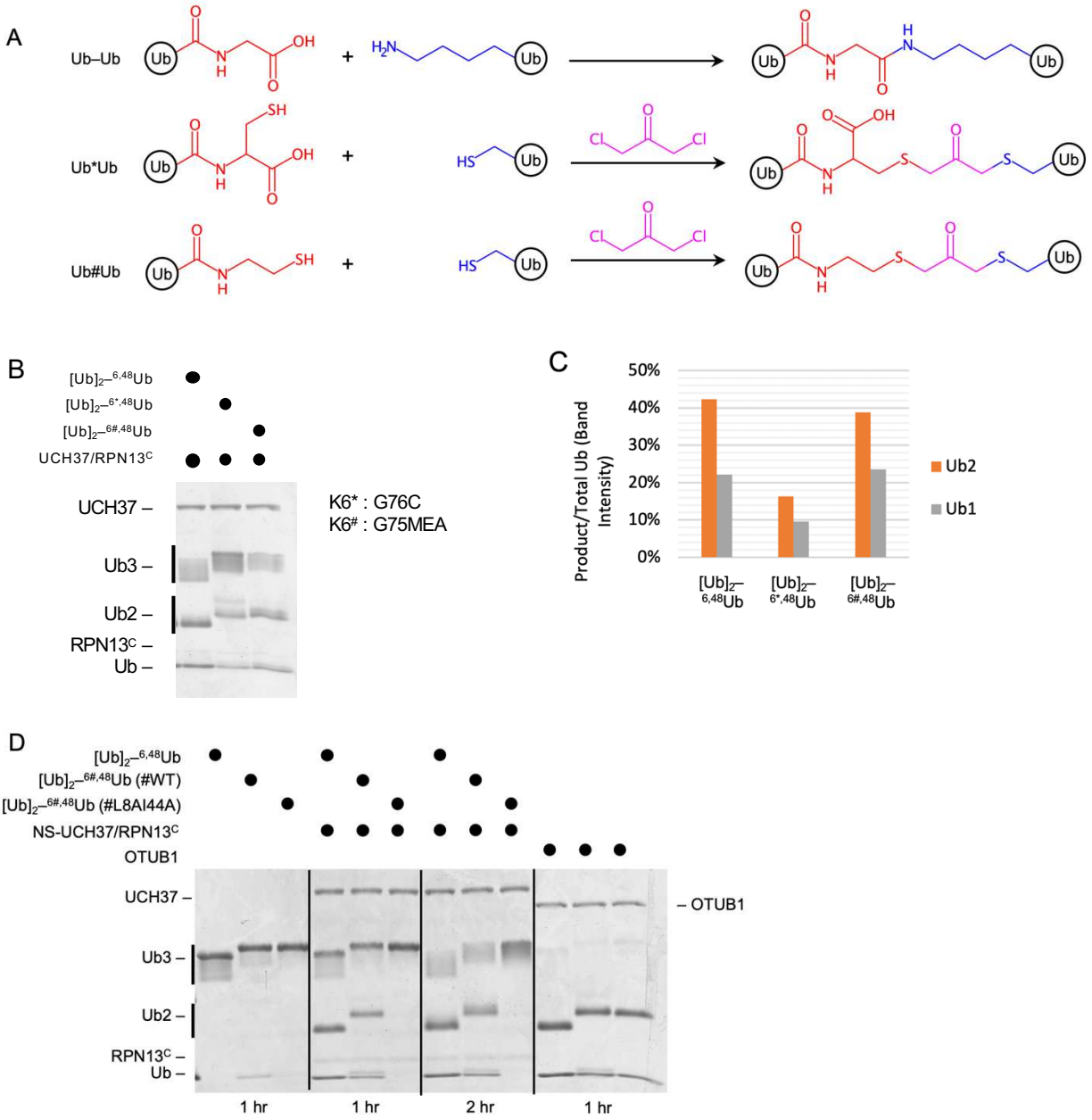

FIG 4.1 The hydrophobic patch on non K48–linked branch Ub is required for UCH37 activity. (A) Chemical structure of a native isopeptide bond compared to the linkages formed using two different crosslinking approaches used in the generation of crosslinked branched chain mimics. (B) Uch37/Rpn13^{C} catalysis of branched Ub chains synthesized using native chain linkage strategies were compared with those synthesized by crosslinking strategies 1 and 2. Reactions of 1 μM Uch37/Rpn13c and 5 μM substrate, incubated for 2 hours were analyzed by SDS-PAGE and quantified as described previously. (C) Quantification of (B) showing products of the Ub2 and Ub1 products of deubiquitination. (D) 5 μM Branched Ub chains generated using crosslinking approach 2, with either distal crosslinked WT Ub or the L8AI44A hydrophobic patch mutant were subject to an in vitro gel-based DUB assay using 1 μM of either NS-Uch37/Rpn13^{C} or the K48-specific DUB Otub1 for 1 and 2 hours at 37ºC. Reactions were quenched and analyzed by SDS-PAGE and Coomassie stain.

proximal Ub (blue), DCA (pink)). Comparing the hydrolysis of 5 μM $[Ub]_2$–^{6,48}Ub to $[Ub]_2$–^{6*,48}Ub by 1 μM Uch37/Rpn13^{C} reveals that Mimic 1 is a far less preferred substrate than the native chain (Fig. 4.1, B & C). In other words, this crosslinked branched chain approach is not suitable to represent the native chain. We predicted this is a result of the additional carboxylic acid within Mimic 1.

Utilizing an approach to modify the C-terminus of Ub via Intein splicing chemistry,[49] we generated Ub containing a C-terminal thiol, but without the carboxylic acid. This strategy was developed by Dr. Robert Cohen (unpublished).This was made possible by expressing Ub as a Ub-Intein-CBD (Chitin binding domain) fusion protein, isolating the protein on chitin affinity resin, and inducing Intein splicing and generation of the desired Ub C-terminus by the addition of mercaptoethylamide (MEA). This Ub_{75}-MEA was then used in the DCA crosslinking reaction with the proximal K6C containing K48-linked Ub dimer to generate Mimic 2: $[Ub]_2$–$^{6\#,48}$Ub (Fig. 4.1, A). Comparing the hydrolysis of 5 μM $[Ub]_2$–^{6,48}Ub to $[Ub]_2$–$^{6\#,48}$Ub by 1 μM Uch37/Rpn13^{C} reveals that Mimic 2 is recognized and hydrolyzed almost identical to the native linked branched Ub chain (Fig. 4.1, B & C), making the second approach suitable for generating crosslinked Ub chains representative of native linked branched chains.

4.3 The Ub hydrophobic patch on the K6-linked Ub in the $[Ub]_2$–^{6,48}Ub branched chain is essential for catalysis by Uch37/Rpn13c

To ask about the importance of the hydrophobic patch on the distal K6-linked Ub within the $[Ub]_2$–^{6,48}Ub branched chain, we used the second crosslinking approach to generate a crosslinked branched chain containing a distal K6-linked hydrophobic patch mutant Ub, denoted as $[Ub]_2$–$^{6\#,48}$Ub ($^{\#}$Ub L8AI44A). Our *in vitro* gel-based Uch37/Rpn13^{C} DUB assay comparing the hydrolysis of $[Ub]_2$–^{6,48}Ub, $[Ub]_2$–$^{6\#,48}$Ub, and $[Ub]_2$–$^{6\#,48}$Ub (#L8AI44A) revealed that while the branched chains containing WT K6-linked Ub are deubiquitinated as expected, there was no observable deubiquitination of the branched chain containing L8AI44A K6-linked Ub (Fig.4.1, D). To prove that this crosslinked mutant branched chain Ub is still hydrolysable at the K48-

linkage, the same chains were shown to be completely cleaved by the K48-linkage specific DUB, OTUB1. These results reveal that the hydrophobic patch on the distal K6-position within the $[Ub]_2$–^{6,48}Ub branched chain is essential for catalysis by Uch37/Rpn13^{C}.

4.4 Discussion

The chemistry of crosslinking using the small molecule DCA allowed us to generate a unique branched Ub chain that could not otherwise be generated by Ub conjugating enzymes. Our initial approaches crosslinking Ub G76C to Ub–^{48}Ub with a proximal K6C Ub produced a branched chain that mimics the native linked $[Ub]_2$–^{6,48}Ub aside from the additional length of a ~1.5Å (A single C–C bond length) and an additional carboxylic acid group. Uch37/Rpn13^{C} DUB assays revealed that $[Ub]_2$–^{6,48}Ub branched chains synthesized using this approach and containing these small differences in structure are not hydrolyzed equivalently to the native linked chains. The second approach crosslinking Ub_{75}-MEA, a Ub with an Intein and MEA-modified C-terminus, to a proximal cysteine containing Ub–^{48}Ub, produced a branched chain identical to the first mimic, but without the additional carboxylic acid produced in the synthesis of Mimic 1. Uch37/Rpn13^{C} hydrolysis of this second branched chain mimic was almost identical to that of the native linked branched Ub chain. This revealed that the presence of the additional negatively charged COO- between the Ub–Ub K6-linkage in the branched Ub chain diminishes the catalytic activity of Uch37/Rpn13^{C}. One possibility for this could be that the additional COO- near the bond causes a repulsive force either due to steric clash or repulsion due to a close proximity of like charges. Equivalent hydrolysis of the branched chain generated with a distal K6-linked Ub_{75}-MEA and the native branched chain confirmed that this approach is necessary for generating crosslinked branched chain mimics that resemble the native branched chains. Once other branched chain specific effectors are discovered, this approach could prove useful to probing structural characteristics of the binding interaction in a similar way as we used here.

Once a Ub L8AI44A Ub_{75}-MEA was generated and used to make a $[Ub]_2$–$^{6\#,48}$Ub, we were able to determine that the hydrophobic interaction between the hydrophobic patch (L8 and

I44) on the distal K6-linked Ub and Uch37 is essential for catalysis. This allowed us to hypothesize that a specific binding interface between the non-hydrolyzed Ub and Uch37 is essential for the correct binding and positioning of branched Ub chains. Since the ASCL also plays a regulatory role in branched chain selection, it is likely that the hydrophobic interaction between the distal K6 Ub and Uch37 assists in positioning the branched chain to simultaneously displace the ASCL and bring the K48 isopeptide bond to the active site. As other UCH family DUBs have regulatory ASCLs, it is possible that this binding interaction is translatable between branched Ub chains and other UCH DUBs. From this analysis we gain the first insight into the molecular characteristics that provide enzyme specificity for branched Ub chains. Further work will need to be done to determine the hydrophobic interface on the Uch37/Rpn13^{C} complex that is necessary for binding to the distal K6 Ub hydrophobic patch.

A limitation to the crosslinking approach is that the full binding interface between branched Ub chains and Uch37/Rpn13^{C} remains unknown. Nevertheless, our studies have still illuminated key components of the branched Ub chain interaction with Uch37/Rpn13^{C}.

4.5 Materials and methods

4.5.1 Synthesis and purification of DCA cross-linked branched Ub chains

The dichloroacetone (DCA) crosslinked branched chain Mimic 1 was synthesized by adding proximal K6C thiol containing Ub–^{48}Ub to Ub G76C in a 50 mM borate buffer with 5 mM TCEP. Freshly prepared 0.1 M DCA dissolved in N,N'-dimethylformamide was then added to a final concentration equal to one half the total concentration of free thiols in solution. Reactions were incubated at 25ºC for 30 minutes and quenched by the addition of 10 mM BME. Crosslinked branched chains were purified the same as the native synthesized poly-Ub chains described above.

Ub75-Intein-CBD (Chitin Binding Domain) was expressed from the pTYB2 His-Ub75-Intein-CBD plasmid and Ub_{75}-MEA was generated by Andy Roddam. To produce the branched Ub chain with a mutated hydrophobic patch on the K6-crosslinked Ub, mutagenesis primers

were used to mutate Ub L8A and I44A within the pTYB2 plasmid and Ub(L8AI44A)$_{75}$-MEA was generated by Justin Curtiss. The fusion protein was expressed, cleaved, and purified the same as the WT. Crosslinking at the proximal K6C on a Ub–^{48}Ub via DCA and subsequent purification was also performed as before.

CHAPTER 5: ESTABLISHING A SYSTEM TO PROBE THE FUNCTION OF PROTEASOME-ASSOCIATED UCH37

5.1 Introduction

Uncovering Uch37 selective activity for branched Ub chains has provided the initial clues for how Uch37 might be regulating ubiquitinated substrates at the proteasome. Our biochemical analysis of Uch37 activity with and without Rpn13 has revealed some key components to the molecular basis of this enzymatic activity. Future studies will seek to understand the function of debranching by Uch37 at the proteasome. To accomplish this, we must establish a system to monitor degradation of linear or branched chain modified substrates by Uch37-bound or Uch37-null proteasomes. The *in vitro* analysis of substrate degradation, monitored by fluorescence anisotropy, will provide insights into the degradation enhancing or inhibiting effects of debranching at the proteasome.

5.2 Strategy for purifying endogenous proteasomes with or without bound Uch37

In order to determine how Uch37 activity at the proteasome affects the degradation of substrates modified with different types of Ub chains, proteasomes must be purified while controlling for the occupancy of Uch37. In order to obtain proteasomes without Uch37, proteasomes were affinity purified from HCT116 Uch37 KO cells using previously determined approaches.[50] This process requires cell lines expressing an HBTH (His tag, Biotinylation signal, TEV cleavage site, His tag) tagged Rpn11 (a gift from Aixin Song). These cells are harvested and the endogenously biotinylated HBTH-Rpn11 is pulled down using streptavidin affinity resin. As Rpn11 is an essential component of functional 26S proteasomes, the affinity pull-down of

HBTH-Rpn11 allows for the purification of whole 26S proteasomes. While proteasomes are bound to the resin, a wash with high salt buffer removes Usp14 from the proteasome.[51] When probing the function of DUBs at the proteasome, removal of Usp14 helps deconvolute the results and allows analysis of DUB activity solely from Uch37 or Rpn11. To the streptavidin resin bound proteasome, TEV protease is added to cleave the proteasome off the resin. 26S proteasomes are then separated from TEV protease, Usp14, and other smaller residual components by ultracentrifugation in a buffer solution containing 20% glycerol. Fractions are taken from top to bottom after ultracentrifugation, and after the last fraction is taken, the pelleted proteasome is resuspended in proteasome storage buffer.

Attempts were made to load Uch37 onto proteasomes by supplementing with recombinant Rpn13 and Uch37 but proved to be unsuccessful. To obtain proteasomes ensuring the presence of Uch37, HEK 293 cells stably transfected with GFP-TEV-Uch37 or GFP-TEV-Uch37(C88S) (gifts from Aixin Song) were harvested and proteasomes were pulled down using affinity resin conjugated with a GFP-nanobody (a gift from Justin Curtiss).[52] Proteasomes were cleaved off of resin using TEV protease, ultracentrifuged, and collected as before. This process was successfully used to purify both WT and catalytically inactive (C88S) Uch37 bound proteasomes. Not all 26S proteasomes contain Uch37, so greater amounts of cells were harvested to obtain close to the amount of proteasome using the GFP pull-down as compared to the initial purification method. Each fraction and the resuspended pellet are analyzed by SDS-PAGE followed by silver stain to determine the purity, and the presence of full 26S proteasomal components (FIG. 5.1, A). The molar concentration of 26S proteasomes was quantified by SYPRO Ruby stain and a comparison to 26S proteasome standard purified from bovine red blood cells (FIG. 5.1, B and E). The concentration of Uch37 and Rpn13 in purified proteasome fractions was determined by comparison to titrated Uch37/Rpn13 standard via SDS-PAGE and western blots against each component (FIG 5.1, C and E). The 19S S1 subunit was used as a loading control.

A

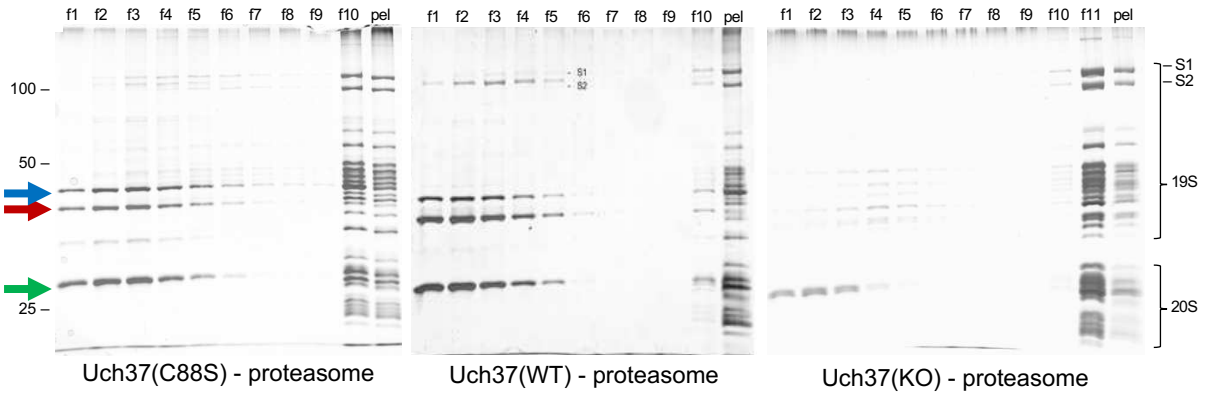

B

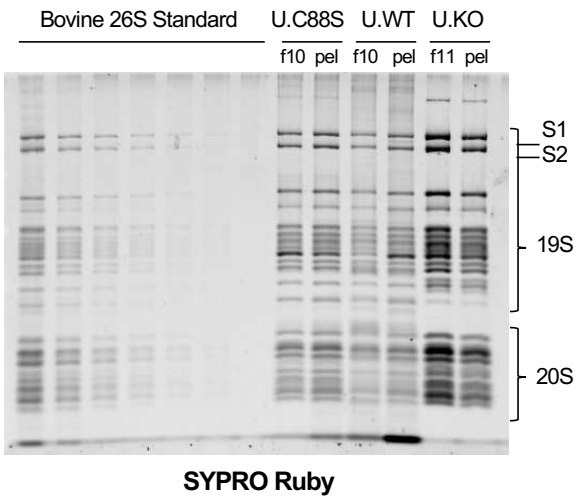

C

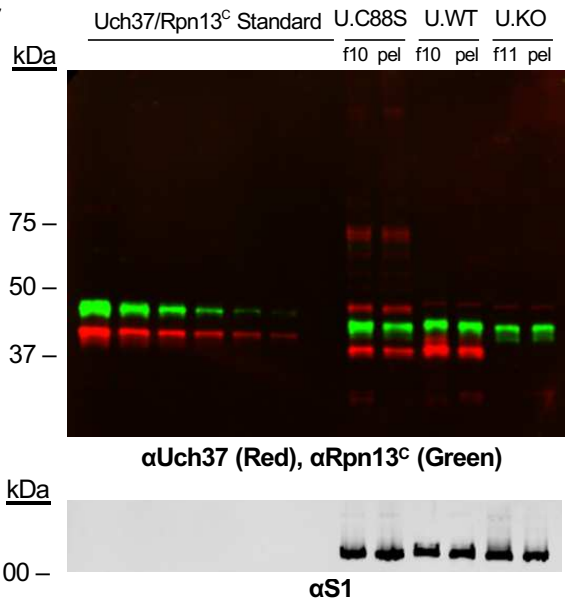

D

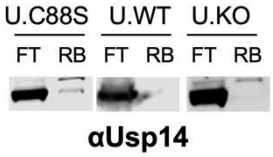

E

Proteasome	Fraction	Concentration		
		26S Proteasome (2X 19S RPs)	Uch37	Rpn13C
Uch37(C88S)	**F10**	0.15 µM	0.20 µM	0.13 µM
	Pellet	0.20 µM	0.19 µM	0.09 µM
Uch37(WT)	**F10**	0.10 µM	0.12 µM	0.06 µM
	Pellet	0.15 µM	0.09 µM	0.09 µM
Uch37(KO)	**F11**	0.47 µM	0	0.15 µM
	Pellet	0.32 µM	0	0.11 µM

FIG 5.1 Purification and characterization of the 26S Proteasome. (A) Uch37(C88S), Uch37(WT), or Uch37(KO) 26S Proteasomes purified from HEK 293 cells or HCT 116 cells were pelleted by ultracentrifugation and the fractions analyzed by SDS-PAGE followed by silver stain. An unidentified protein (blue), Uch37 (red), and TEV protease (green) are shown with arrows as the primary components removed by the glycerol ultracentrifugation step. (B) Purified proteasome concentration was determined by comparison to a 26S proteasome standard from bovine red blood cells. Samples were stained using SYPRO Ruby gel stain. (C) Uch37 and $Rpn13^{C}$ concentration in each purified proteasome sample was quantified by SDS-PAGE and western blot against recombinant Uch37/$Rpn13^{C}$ standards. The proteasome 19S subunit S1 was used as a loading control. (D) Western blot against Usp14 for each sample taken after proteasome resin-bound wash and before TEV protease cleavage. FT, flow through wash and RB, resin bound proteasome. (E) Proteasome, Uch37, and $Rpn13^{C}$ molar concentration is presented for each proteasome fraction and for each proteasome type.

5.3 Using a domain of the mega protein Titin as a model substrate for branched chain modification and proteasome degradation

The second component needed to monitor proteasomal degradation *in vitro* is an appropriate model substrate. Bard J.A.M. et al engineered the Immunoglobulin-like I27 subdomain of the mega protein Titin to include the necessary components of a proteasome substrate: a folded domain whose stability can be tuned by the introduction of destabilizing mutations, a terminally unstructured region for engaging with the proteasomal ATPases, a controlled number of lysines, a PY motif for recognition by Ub conjugating enzymes, and a cysteine for labeling with a fluorophore via maleimide chemistry.[53, 54] This protein will be expressed purified, labeled with a fluorophore, and eventually modified with pre-made linear or branched poly-Ub chains of defined linkages. Having the substrate labelled with a fluorophore allows for monitoring of degradation by the proteasome by fluorescence anisotropy because the mass difference between unbound substrate, proteasome bound substrate, and the resulting small proteolyzed peptides are large.

5.4 Strategy for pentameric Ub chain synthesis

In order to ask questions about debranching by Uch37 at the proteasome, our fluorophore-labelled model substrate will be conjugated with either linear or branched Ub

chains. A model for substrate engagement by the proteasome has been proposed where the longer a ubiquitinated substrate can stay associated with the proteasome, the more likely the substrate will engage with the proteasomal AAA ATPase and be threaded into the degradative core.[55] Since Ub binding to each Ub receptor has relatively high on and off rates, it is important for ubiquitinated substrate to "sample" multiple receptors to increase retention time. For this reason, substrates modified with four or more Ub molecules have been shown to be better targets for proteasomal degradation.[55, 56] With this in mind, we synthesized three types of poly-Ub chains composed of five total ubiquitins (pentameric Ub chains): K48-linked linear Ub5, K48-linked Ub5 containing a proximal K6/K48-linked branched Ub chain, and K48-linked Ub5 containing a distal K6/K48-linked branched Ub chain.

A strategy has been established to build all three pentamer Ub chains in a stepwise fashion using three Ub monomers: K6RK48RK63R Ub, K6RK48CK63R Ub, and K63R Ub(D77) (Fig. 5.2).[28] Since we are using the K63-linkage specific E3 ligase Rsp5 to ligate each of our pre-built chains to the model substrate, each ubiquitin used in the pentamer synthesis has the K63 position blocked by a K63R mutation to prevent Rsp5 from building chains at that position. Using the K48-specific E2 conjugating enzyme Cdc34 and the K6/K48-linkeage directing E3 ligase NleL, each dimer, trimer, or pentamer will be built blocking undesirable points of conjugation using Lys to Arg mutations where indicated. For one monomer, the K48 position was blocked using a Lys to Cys mutation, so in later steps this position can be deblocked using a cysteine to amino ethyl cysteine (AEC) conversion step. This reaction utilizes the small molecule azridine which reacts with the cysteine thiol, opening the azridine ring, leaving the previously blocked residue with a primary amine containing residue the size and shape of lysine. Conjugating enzymes can then use this AEC as a point of Ub conjugation. Another blocking/deblocking strategy was used at the Ub C-terminus where applicable. The C-terminal D77 effectively blocked the proximal Ub and, when necessary, the C-terminal D77 was deblocked by cleaving if off with the DUB YUH1.

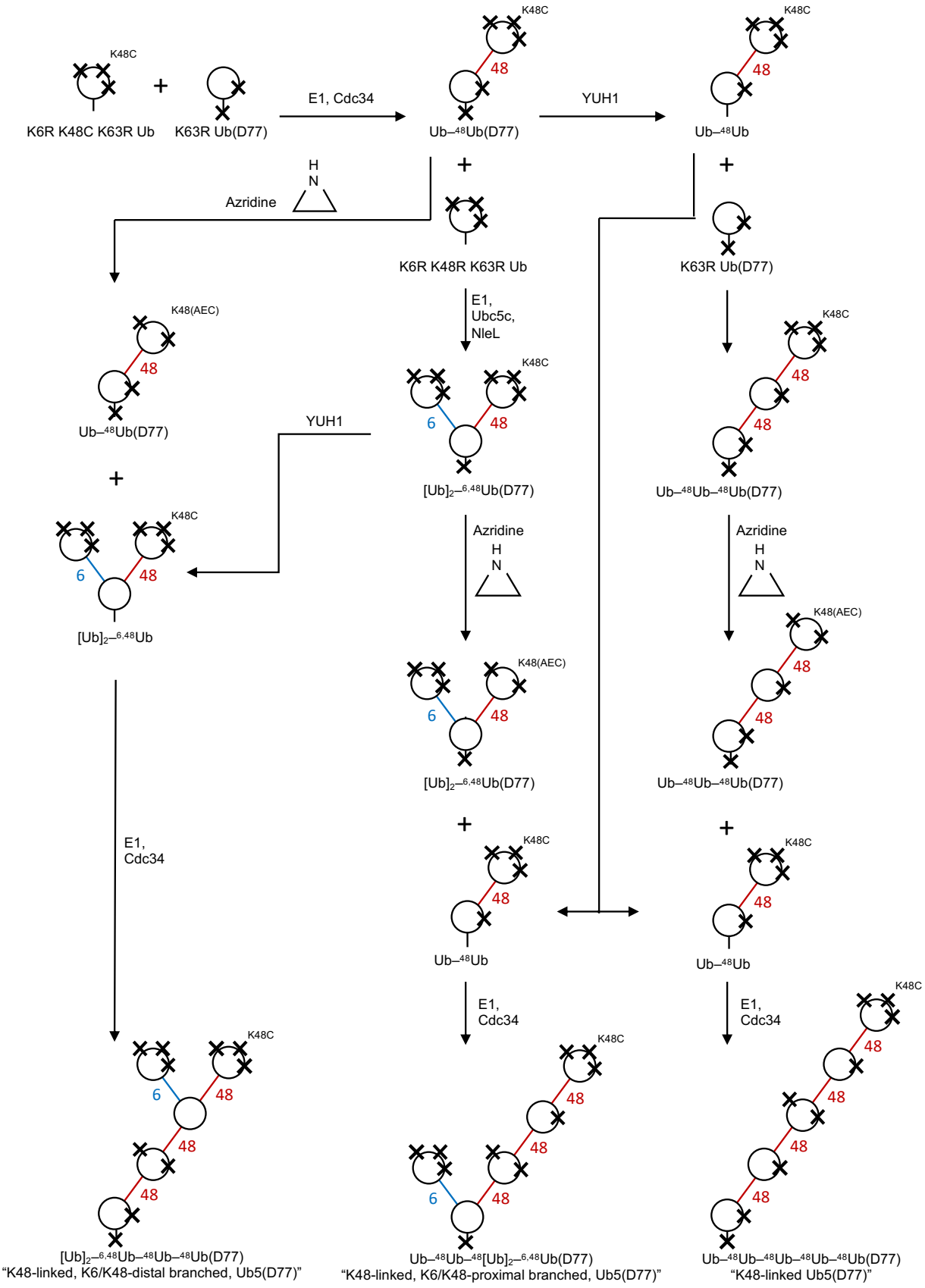
K48C
K6R K48C K63R Ub
K63R Ub(D77)
E1, Cdc34
Ub–48Ub(D77)
YUH1
Ub–48Ub
Azridine
H
N
K6R K48R K63R Ub
K63R Ub(D77)
K48(AEC)
Ub–48Ub(D77)
E1,
Ubc5c,
NleL
[Ub]2–6,48Ub(D77)
Ub–48Ub–48Ub(D77)
[Ub]2–6,48Ub
E1,
Cdc34
Ub–48Ub
[Ub]2–6,48Ub–48Ub–48Ub(D77)
"K48-linked, K6/K48-distal branched, Ub5(D77)"
Ub–48Ub–48[Ub]2–6,48Ub(D77)
"K48-linked, K6/K48-proximal branched, Ub5(D77)"
Ub–48Ub–48Ub–48Ub–48Ub(D77)
"K48-linked Ub5(D77)"

FIG 5.2 Pentameric Ub chain synthesis strategy. Pentameric branched or linear Ub chains were generated using this stepwise synthesis strategy. Each poly-Ub chain was synthesized starting from three types of monoUb: K6R K48R K63R Ub, K6R K48C K63R Ub, and K63R Ub(D77). Where applicable, blocked K48C conjugation points were deblocked by conversion to amino ethyl cysteine by reaction with aziridine. Chains were purified after each synthesis step as described in materials and methods.

5.5 Discussion

Each fluorophore labeled substrate will be prepared and conjugated with a single type of either branched or linear pentameric Ub chain. The degradation of each type of ubiquitinated substrate will be monitored by Uch37-bound, Uch37(C88A)-bound, or Uch37-null 26S proteasomes. The degradation of each substrate by Uch37-null proteasomes will establish a baseline for the degradation rate of each type of ubiquitinated substrate in the absence of Uch37. The addition of Uch37 and presumably branched Ub chain specific deubiquitinating activity will reveal how debranching affects the rates of degradation. Degradation rates observed between the WT and C88S Uch37-bound proteasomes will highlight the differences in proteasomal substrate processing that are solely due to the activity of Uch37, as opposed to both the catalytic activity and Ub chain binding. Comparison of the Uch37(C88S) and Uch37-null proteasomes will reveal any regulatory contribution Uch37 might provide that is not dependent on its catalytic activity.

Given that Uch37 has higher binding affinity for K6/K48-linked branched Ub chains over other types of Ub chains, the addition of Uch37's Ub binding ability to the proteasome might provide an increase in the substrate recruitment capacity of the proteasome for branched chain substrates. This would lead to enhanced recruitment of branched Ub chain modified substrates over linear Ub chain modified substrates seen between Uch37-null and Uch37(C88S)-bound proteasomes.

The contribution of debranching to substrate processing by Uch37 and proteasome could have a number of different possible effects. It is possible that the position of the branched chain (proximal or distal) on the substrate could allow for differences in the fates of the

substrate. Debranching of the proximal Ub chain would produce a substrate with only a Ub–^{6}Ub remaining, whereas debranching of the distal Ub chain would produce a substrate leave a Ub–^{6}Ub–^{48}Ub–^{48}Ub chain. If this debranching activity occurred prior to substrate engagement, the Uch37 "processed" substrate left with only the Ub dimer would be more difficult to retain than the chain left with a Ub tetramer, leading to the release or "rescue" of the proximally branched Ub chain modified substrate.

If debranching occurred after substrate engagement, then it is possible that the catalytic activity of Uch37 could assist in editing an existing branched chain to make it a more suitable substrate for hydrolysis by Rpn11. Rpn11 sits above the entry channel of the 19S regulatory particle, removing Ub and whole Ub chains from substrates to allow for proper polypeptide translocation. It is possible that branched chains, specifically proximal branched chains (those closer to the site of Rpn11 hydrolysis), could be harder to cleave by Rpn11. If this were the case, degradation of the proximally branched chain modified substrate would be faster in a Uch37-bound proteasome context compared to a Uch37-null context. It would also need to be shown that in a Uch37-null proteasome context, the proximally branched Ub modified substrates are degraded slower than the distally branched Ub modified substrates for this proposal to be accurate.

Another possible function of Uch37 activity at the proteasome could be to decrease the product inhibition caused by long poly-Ub chains that remain bound to proteasomal Ub receptors even after they have been released from their substrate. If this were happening, long poly-Ub chains could occupy proteasomal Ub binding positions for periods of time after substrate degradation preventing the binding and degradation of further substrates. It is possible that in a Uch37-bound proteasome context, Uch37 could be "trimming" long Ub chains to assist in their release and the availability of incoming proteasome-targeted substrates. This possibility could be viewed in our *in vitro* degradation assays as enhanced catalysis of branched chain

modified substrates in a WT Uch37-bound context over that with Uch37(C88S) and without Uch37 at all.

It is also possible that the initial results could show no difference in substrate degradation between any type of Ub chain modified substrate and any proteasome type. If this were the case, it could be due to the substrate being degraded faster than Uch37 hydrolysis, making it difficult to distinguish the different effects of branched Ub chain hydrolysis. Thankfully, the stability of our model substrate has the ability to be tuned. Based on the finding that the protein unfolding is the rate limiting step of proteasomal degradation, we could increase the stability of our substrate if necessary to increase the time of degradation and hopefully observe differences in substrate processing due to Uch37 activity.[44] Despite potential difficulties, the system we've established is a versatile system with the potential to uncover important characteristics of the function of Uch37 at the proteasome.

5.6 Materials and methods

5.6.1 Antibodies

The following antibodies were used: The mouse anti-Uch37 monoclonal antibody (SantaCruz, sc-271002), The rabbit anti-STI136(Rpn13) antibody (Made in our lab), The rabbit anti-proteasome 19S subunit S1/Rpn2 antibody (Boston Biochem, AP-104), and The rabbit anti-Usp14 antibody (Bethyl Laboratories, A300-920A).

The GFP-nanobody was purified by another member of the lab according to the established protocol.[52]

5.6.2 Cell culture

GFP-Uch37 HEK 293 cells were generated by Tingting Yao and the Uch37 KO HBTH-Poh1 cells were generated by Aixin Song. HEK 293 cells were cultured in DMEM, and HCT 116 cells were cultured in McCoy's 5a medium, both of which were supplemented with 10% FBS, 100 U/ml penicillin-streptomycin, and 2 mM L-glutamine. Cells were grown and expended to obtain 15 or more, 15 cm plates of cells. For the cells containing Uch37 under a

Doxycyclin/Tetracyclin inducible promoter, gene expression was induced with 1 µg/ml Tet and cells were grown for 48 hours longer. When cells reached at 80-90% confluence, the cells were harvested. The media in each plate was aspirated, the cells were washed twice with chilled 1X PBS, and the cells were gently scraped from the dish using a cell scraper. Cells were combined, transferred to 15 ml falcon tubes, and pelleted by centrifugation at 800 rpm, 4ºC, for 3 minutes.

5.6.3 Proteasome Purification

The day of harvest, cells were lysed, and the cytosolic extract was isolated and stored at -80º till proteasome purification. For cell lysis, 1 ml of cytosolic extract lysis buffer (50 mM NaPi, pH 7.5, 200 mM NaCl, 5 mM $MgCl_2$, 0.5% NP40, 5 mM ATP, 1 mM DTT, and 10X proteasome inhibitor cocktail (Sigma #P8340)) per 15 cm dish was added to the pelleted cells. Cell lysis was achieved by passing the resuspended cells through a 21G needle 20 times. Lysed cells were incubated on ice for 15 minutes, then spun at 13,000 rpm, 4ºC, for 15 minutes. The cytosolic extract was collected, and 10 µl was used in a Bradford assay to determine total soluble protein content. The remaining cytosolic extract was flash frozen in liquid nitrogen and stored at -80ºC.

For purification of HBTH-Rpn11 proteasomes, 10 µl streptavidin affinity resin (cat #20353)/mg total soluble protein was equilibrated in ≥ 10 resin bed volumes of cytosolic extract lysis buffer. Cytosolic extract was added to the resin and incubated for 2 hours at 4ºC. Resin was spun at 2500 g for 2 minutes, and the supernatant was removed. The resin bed was washed with lysis buffer (≥20 bed volumes total; the step to remove Usp14), rotated at 4ºC for 10 minutes, spun, supernatant was removed, and the wash was repeated. The resin was buffer exchanged into TEV protease buffer (20 mM Tris pH 7.6, 5 mM $MgCl_2$, 50 mM NaCl, 1 mM EDTA, 5% glycerol, 5 mM ATP, and 1 mM DTT) the same as the above washes. 300 µl TEV cleavage buffer was added to each resin bed, then 2.2 µg TEV protease per 15 cm plate of cells was added to the buffer suspended resin bed. TEV cleavage was allowed to occur while gently rotating at room temperature for 4 hours. TEV cleaved proteasome-resin solution was pelleted as before and the supernatant containing the affinity purified proteasome was collected. The

resin was washed two more times with half of a resin bed volume of buffer, samples were pelleted, and the supernatant was collected together. 1 mM AEBSF was added to the proteasome sample to inactivate TEV protease. The sample was passed through a benchtop spin column to separate any residual resin.

Prior to the final purification step, silver stain and western blots of samples taken during the initial steps of purification were done to ensure the absence of Usp14, sufficient proteasome pulldown, and complete cleavage of proteasome from resin.

Finally, proteasomes were subjected to glycerol density ultracentrifugation to separate proteasome samples from free Uch37, TEV protease, and other small impurities. 2.2 ml TEV buffer containing 20% glycerol was added to Beckman Coulter 3.5 ml open-top thickwall polypropylene ultracentrifuge tubes and 700 µl of the eluted proteasome solution was gently layered on top of the 20% glycerol buffer. Ensuring an appropriate counterbalance, the proteasome was centrifuged in a Beckman Optima TL 100 Ultracentrifuge at 4ºC, 70k rpm, for 2.3 hours. Afterward 300 µl fractions were taken from the top to bottom, and the pellet was resuspended in 100 µl TEV buffer. All fractions were analyzed by silver stain to ensure appropriate pelleting of the proteasome and to collect the samples containing pure proteasome (FIG. 5.1, A). Samples were flash frozen and stored at -80ºC.

Proteasomes from cells expressing GFP-TEV-Uch37 (WT or C88S) were purified similarly, except resin conjugated with GFP-nanobody was used to immunoprecipitate Uch37-bound proteasomes. Where applicable, 3.1 µl resin/mg total protein was used in place of streptavidin resin.

All proteasome samples post-glycerol ultracentrifugation were run together on SDS-PAGE alongside titrating concentrations of a bovine 26S proteasome standard. The gel was stained using a SYPRO Ruby staining method. Two standard curves were established from the S1 band and the sum of all the 20S bands and used to measure the molar concentration of each purified proteasome sample (FIG. 5.1, B). To determine the amount of Uch37 and Rpn13

in each of the purified proteasome samples, each proteasome sample was run as before on SDS-PAGE, but alongside a co-purified NS-Uch37/Rpn13^{C} standard. The resulting gel was subject to western blot using αUch37 (Ms), αRpn13 (Rb) antibodies, and αS1 (Rb) antibodies. The S1 signal was used as a loading control and the concentrations of Uch37 and Rpn13 in each proteasome sample were determined from the standard curve (FIG. 5, C). All values determined of proteasome, Uch37, and Rpn13 concentrations are displayed together in FIG. 5, D.

5.6.4 Synthesis of pentameric branched Ub chains

The desired pentameric Ub chains were built from three Ub mutants: K6RK48RK63R Ub, K6RK48CK63R Ub, and K63R Ub(D77). The K6RK48RK63R Ub monomer was generated by site specific mutagenesis of K63R in the pET3a-Ub(K6RK48R) plasmid. The K6RK48CK63R Ub monomer was generated by site specific mutagenesis of R48C in the pET3a-Ub(K6RK48RK63R) plasmid. The K63R Ub(D77) monomer was generated by site specific mutagenesis of K63R in the pET3a-Ub(D77) plasmid. Each plasmid was expressed in BL21(DE3) cells and purified as described earlier.

Where indicated, two ubiquitins were covalently linked at K48 by the Ub conjugation reaction using E1 and the K48-linkage directing E2, Cdc34. The single branched chain formed in this pentamer synthesis strategy was made by conjugating K6RK48RK63R Ub to the proximal K6 Ub position on a K48 dimer using E1, Ubc5c (E2), and Nlel (E3). In order to deblock proximal positions and generate Ub that can act as a donor, the DUB YUH1 was used to cleave the proximal D77 as described previously.[28] To deblock the distal K48C positions, 55 mM azridine was added to 0.1-1.0 mM cysteine containing poly-Ub chain to generate the primary amine containing aminoethyl cysteine K48(AEC). After incubation at room temperature for 30+ minutes, reactions were quenched with 100 mM BME and dialyzed against 10 mM Tris, pH 7.6 at 4ºC overnight. Post dialysis samples were collected, the concentration was measured, and each were stored at -80ºC. After each Ub conjugation reaction, the desired product was

purified as described previously and prepared for the next steps of conjugation until the desired pentameric chains were made. These chains were prepared with the help of Jeremy Dortch.

5.7 Thesis summary

Uch37 is a highly conserved deubiquitinating enzyme that binds to the 19S regulatory component of the proteasome via Rpn13 and assists in the regulation of proteasomal degradation by processing ubiquitinated substrates. Despite its important role in cell cycle regulation, early embryonic development, and its potential as a drug target for treatment of cancers, the function of Uch37 at the proteasome has remained elusive. This project has begun by identifying the *in vitro* substrate specificity of Uch37 alone and bound to the proteasomal subunit Rpn13. We determined that Uch37 has a high degree of specificity and activity for branched Ub chains over Ub chains of linear topologies. We identified the K48 linkage-specific activity of Uch37/Rpn13, leading to our understanding of Uch37 possessing “debranching” activity. We showed that Rpn13 assists in this branched Ub chain selection through stabilizing contacts with the ASCL of Uch37. This stabilizing effect prohibits the catalysis of linear Ub chains and helps to select for branched Ub chain substrates. Understanding the conservation between UCH family DUBs we propose that our various *in vitro* analytical methods might prove useful in the understanding of the activity of other UCH family enzymes.

To better understand the kinetics of substrate recognition and catalysis, we characterized the binding affinity of Uch37/Rpn13^{C} toward different poly-Ub chain types as well as solved the Michaelis-Menten kinetic parameters of Uch37/Rpn13^{C} for various branched chain types. From this information we were able to conclude that for one branched chain type, Uch37/Rpn13^{C} had a 5- to 10-fold higher binding affinity over all of the other Ub chain types. It was also shown that the binding affinity for the other branched chain types measured was similar to that for the linear Ub chain types. Seeing from the gel-based assays how branched Ub chains are cleaved far greater than the linear chains however, we conclude that the branched Ub chain topology is necessary for catalysis. Our Michaelis-Menten kinetic analysis revealed

that branched chains linked via K11/K48 are cleaved by Uch37/Rpn13 the fastest. Determination of the catalytic efficiency (k_{cat}/K_M) revealed values that were very similar between K6/K48-linked and K11/K48- linked branched chains, revealing both of these Ub chain types as viable substrates for Uch37/Rpn13. This analysis also showed that the K63/K48-linked branched Ub chain, despite possessing a branched chain topology, is not a favorable substrate for Uch37. This shows that not only are branched chains necessary for Uch37/Rpn13 catalysis, but the positioning of the branches is also important for selection and catalysis of substrates.

These results led to questions regarding the structural determinants of branched Ub chain selection and catalysis. Using the $[Ub]_2$–^{6,48}Ub branched chain as a model substrate, we proposed that some feature of the non-K48-linked, i.e. the non-hydrolyzed Ub, in the branched Ub chain provides the component necessary to select for branched Ub chains. Through the use of cysteine thiol crosslinking via DCA and the establishment of a cross-linked branched Ub chain mimic that appropriately represents the native-linked branched chain, we were able to deduce that the hydrophobic patch on the non-hydrolyzed Ub in the branched chain is essential for catalysis. Disruption of this hydrophobic patch by replacing L8 and I44 with alanine on the K6-linked Ub prevented any observable degree of deubiquitination by Uch37/Rpn13.

These results provide the foundation for our understanding of Uch37 at the proteasome. With this information we have proposed various functions of Uch37 at the proteasome as it relates to substrate degradation. We have established a system to probe these possible functions that include purified proteasomes with or without Uch37, a model substrate with positions for labeling with a fluorophore and conjugating with poly-Ub chains, as well as pentameric branched or linear Ub chains to test how debranching by Uch37 at the proteasome affects substrate degradation.

5.8 Closing statement

Intracellular ubiquitination and deubiquitination has been established as a complex mode of cellular regulation with roles in the majority of cellular functions. One of the primary functions

of ubiquitination is to tag proteins for degradation by the proteasome, the molecular machine responsible for the majority of intracellular protein degradation. With essential roles in the cell cycle, apoptosis, and the degradation of misfolded proteins, as well as severe pathologies that occur with its dysfunction, the proteasome must be tightly regulated. Our work has assisted in uncovering the regulatory contribution of Uch37, one of the three intrinsic deubiquitinating enzymes associated with the 26S proteasome. The DUB Uch37 is the first enzyme discovered to possess branched Ub chain specific activity. As the complexity of the Ub code is progressively being uncovered, this finding provides evidence for the existence of Ub effectors that possess substrate specificity not only dependent on the linkage type but the topology of the poly-Ub signal as well. From our work not only have we provided a greater understanding of a key piece of cellular proteostasis as it relates to proteasomal degradation, but we have also assisted in the further deciphering of the Ub code.

REFERENCES

[1] de Poot, S. A. H., Tian, G., and Finley, D. (2017) Meddling with Fate: The Proteasomal Deubiquitinating Enzymes, *J Mol Biol 429*, 3525-3545.

[2] Komander, D. (2009) The emerging complexity of protein ubiquitination, *Biochem Soc Trans 37*, 937-953.

[3] Eddins, M. J., Varadan, R., Fushman, D., Pickart, C. M., and Wolberger, C. (2007) Crystal structure and solution NMR studies of Lys48-linked tetraubiquitin at neutral pH, *J Mol Biol 367*, 204-211.

[4] Weeks, S. D., Grasty, K. C., Hernandez-Cuebas, L., and Loll, P. J. (2009) Crystal structures of Lys-63-linked tri- and di-ubiquitin reveal a highly extended chain architecture, *Proteins 77*, 753-759.

[5] Paul, S. (2008) Dysfunction of the ubiquitin-proteasome system in multiple disease conditions: therapeutic approaches, *Bioessays 30*, 1172-1184.

[6] Boughton, A. J., Krueger, S., and Fushman, D. (2019) Branching via K11 and K48 Bestows Ubiquitin Chains with a Unique Interdomain Interface and Enhanced Affinity for Proteasomal Subunit Rpn1, *Structure*.

[7] Erpapazoglou, Z., Walker, O., and Haguenauer-Tsapis, R. (2014) Versatile roles of k63-linked ubiquitin chains in trafficking, *Cells 3*, 1027-1088.

[8] Grice, G. L., and Nathan, J. A. (2016) The recognition of ubiquitinated proteins by the proteasome, *Cell Mol Life Sci 73*, 3497-3506.

[9] Kim, H. T., Kim, K. P., Lledias, F., Kisselev, A. F., Scaglione, K. M., Skowyra, D., Gygi, S. P., and Goldberg, A. L. (2007) Certain pairs of ubiquitin-conjugating enzymes (E2s) and ubiquitin-protein ligases (E3s) synthesize nondegradable forked ubiquitin chains containing all possible isopeptide linkages, *J Biol Chem 282*, 17375-17386.

[10] Meyer, H. J., and Rape, M. (2014) Enhanced protein degradation by branched ubiquitin chains, *Cell 157*, 910-921.

[11] Yau, R. G., Doerner, K., Castellanos, E. R., Haakonsen, D. L., Werner, A., Wang, N., Yang, X. W., Martinez-Martin, N., Matsumoto, M. L., Dixit, V. M., and Rape, M. (2017) Assembly and Function of Heterotypic Ubiquitin Chains in Cell-Cycle and Protein Quality Control, *Cell 171*, 918-933 e920.

[12] Liu, C., Liu, W., Ye, Y., and Li, W. (2017) Ufd2p synthesizes branched ubiquitin chains to promote the degradation of substrates modified with atypical chains, *Nat Commun 8*, 14274.

[13] Ohtake, F., Saeki, Y., Ishido, S., Kanno, J., and Tanaka, K. (2016) The K48-K63 Branched Ubiquitin Chain Regulates NF-kappaB Signaling, *Mol Cell 64*, 251-266.

[14] Rock, K. L., Gramm, C., Rothstein, L., Clark, K., Stein, R., Dick, L., Hwang, D., and Goldberg, A. L. (1994) Inhibitors of the proteasome block the degradation of most cell proteins and the generation of peptides presented on MHC class I molecules, *Cell 78*, 761-771.

[15] Bard, J. A. M., Goodall, E. A., Greene, E. R., Jonsson, E., Dong, K. C., and Martin, A. (2018) Structure and Function of the 26S Proteasome, *Annu Rev Biochem 87*, 697-724.

[16] Sharon, M., Taverner, T., Ambroggio, X. I., Deshaies, R. J., and Robinson, C. V. (2006) Structural organization of the 19S proteasome lid: insights from MS of intact complexes, *PLoS Biol 4*, e267.

[17] Olszewski, M. M., Williams, C., Dong, K. C., and Martin, A. (2019) The Cdc48 unfoldase prepares well-folded protein substrates for degradation by the 26S proteasome, *Commun Biol 2*, 29.

[18] Zientara-Rytter, K., and Subramani, S. (2019) The Roles of Ubiquitin-Binding Protein Shuttles in the Degradative Fate of Ubiquitinated Proteins in the Ubiquitin-Proteasome System and Autophagy, *Cells 8*.

[19] Yao, T., and Cohen, R. E. (2002) A cryptic protease couples deubiquitination and degradation by the proteasome, *Nature 419*, 403-407.

[20] Song, Y., Li, S., Ray, A., Das, D. S., Qi, J., Samur, M. K., Tai, Y. T., Munshi, N., Carrasco, R. D., Chauhan, D., and Anderson, K. C. (2017) Blockade of deubiquitylating enzyme Rpn11 triggers apoptosis in multiple myeloma cells and overcomes bortezomib resistance, *Oncogene 36*, 5631-5638.

[21] Lee, B. H., Lu, Y., Prado, M. A., Shi, Y., Tian, G., Sun, S., Elsasser, S., Gygi, S. P., King, R. W., and Finley, D. (2016) USP14 deubiquitinates proteasome-bound substrates that are ubiquitinated at multiple sites, *Nature 532*, 398-401.

[22] Bashore, C., Dambacher, C. M., Goodall, E. A., Matyskiela, M. E., Lander, G. C., and Martin, A. (2015) Ubp6 deubiquitinase controls conformational dynamics and substrate degradation of the 26S proteasome, *Nat Struct Mol Biol 22*, 712-719.

[23] VanderLinden, R. T., Hemmis, C. W., Schmitt, B., Ndoja, A., Whitby, F. G., Robinson, H., Cohen, R. E., Yao, T., and Hill, C. P. (2016) Structural Basis for the Activation and Inhibition of the UCH37 Deubiquitylase, *Mol Cell 61*, 487.

[24] Chen, Y., Fu, D., Xi, J., Ji, Z., Liu, T., Ma, Y., Zhao, Y., Dong, L., Wang, Q., and Shen, X. (2012) Expression and clinical significance of UCH37 in human esophageal squamous cell carcinoma, *Dig Dis Sci 57*, 2310-2317.

[25] Randles, L., Anchoori, R. K., Roden, R. B., and Walters, K. J. (2016) The Proteasome Ubiquitin Receptor hRpn13 and Its Interacting Deubiquitinating Enzyme Uch37 Are Required for Proper Cell Cycle Progression, *J Biol Chem 291*, 8773-8783.

[26] Liu, D., Song, Z., Wang, X., and Ouyang, L. (2020) Ubiquitin C-Terminal Hydrolase L5 (UCHL5) Accelerates the Growth of Endometrial Cancer via Activating the Wnt/beta-Catenin Signaling Pathway, *Front Oncol 10*, 865.

[27] Zhang, X., Linder, S., and Bazzaro, M. (2020) Drug Development Targeting the Ubiquitin-Proteasome System (UPS) for the Treatment of Human Cancers, *Cancers (Basel) 12*.

[28] Pickart, C. M., and Raasi, S. (2005) Controlled synthesis of polyubiquitin chains, *Methods Enzymol 399*, 21-36.

[29] Hamazaki, J., Iemura, S., Natsume, T., Yashiroda, H., Tanaka, K., and Murata, S. (2006) A novel proteasome interacting protein recruits the deubiquitinating enzyme UCH37 to 26S proteasomes, *Embo J 25*, 4524-4536.

[30] Michel, M. A., Swatek, K. N., Hospenthal, M. K., and Komander, D. (2017) Ubiquitin Linkage-Specific Affimers Reveal Insights into K6-Linked Ubiquitin Signaling, *Mol Cell 68*, 233-+.

[31] Wiener, R., Zhang, X., Wang, T., and Wolberger, C. (2012) The mechanism of OTUB1-mediated inhibition of ubiquitination, *Nature 483*, 618-622.

[32] Deol, K., Crowe, S., Du, J., Bisbee, H., Guenette, R., and Strieter, E. R. (2020) Proteasome-Bound UCH37 Debranches Ubiquitin Chains to Promote Degradation, *bioRxiv preprint*.

[33] Hanpude, P., Bhattacharya, S., Kumar Singh, A., and Kanti Maiti, T. (2017) Ubiquitin recognition of BAP1: understanding its enzymatic function, *Biosci Rep 37*.

[34] Jensen, D. E., Proctor, M., Marquis, S. T., Gardner, H. P., Ha, S. I., Chodosh, L. A., Ishov, A. M., Tommerup, N., Vissing, H., Sekido, Y., Minna, J., Borodovsky, A., Schultz, D. C., Wilkinson, K. D., Maul, G. G., Barlev, N., Berger, S. L., Prendergast, G. C., and Rauscher, F. J., 3rd. (1998) BAP1: a novel ubiquitin hydrolase which binds to the BRCA1 RING finger and enhances BRCA1-mediated cell growth suppression, *Oncogene 16*, 1097-1112.

[35] Long, L., Furgason, M., and Yao, T. T. (2014) Generation of nonhydrolyzable ubiquitin-histone mimics, *Methods 70*, 134-138.

[36] Berndsen, C. E., and Wolberger, C. (2011) A spectrophotometric assay for conjugation of ubiquitin and ubiquitin-like proteins, *Anal Biochem 418*, 102-110.

[37] Choi, Y. S., Wu, K., Jeong, K., Lee, D., Jeon, Y. H., Choi, B. S., Pan, Z. Q., Ryu, K. S., and Cheong, C. (2010) The human Cdc34 carboxyl terminus contains a non-covalent ubiquitin binding activity that contributes to SCF-dependent ubiquitination, *J Biol Chem 285*, 17754-17762.

[38] Choi, Y. S., Bollinger, S., Prada, L. F., Scavone, F., Yao, T., and Cohen, R. E. (2019) High-affinity free ubiquitin sensors as quantitative probes of ubiquitin homeostasis and deubiquitination, *bioRxiv*.

[39] Hofmann, R. M., and Pickart, C. M. (1999) Noncanonical MMS2-encoded ubiquitin-conjugating enzyme functions in assembly of novel polyubiquitin chains for DNA repair, *Cell 96*, 645-653.

[40] Bremm, A., Freund, S. M., and Komander, D. (2010) Lys11-linked ubiquitin chains adopt compact conformations and are preferentially hydrolyzed by the deubiquitinase Cezanne, *Nat Struct Mol Biol 17*, 939-947.

[41] Lin, D. Y., Diao, J., Zhou, D., and Chen, J. (2011) Biochemical and structural studies of a HECT-like ubiquitin ligase from Escherichia coli O157:H7, *J Biol Chem 286*, 441-449.

[42] Studier, F. W. (2005) Protein production by auto-induction in high density shaking cultures, *Protein Expr Purif 41*, 207-234.

[43] Morrow, M. E., Morgan, M. T., Clerici, M., Growkova, K., Yan, M., Komander, D., Sixma, T. K., Simicek, M., and Wolberger, C. (2018) Active site alanine mutations convert deubiquitinases into high-affinity ubiquitin-binding proteins, *EMBO Rep 19*.

[44] Bard, J. A. M., Bashore, C., Dong, K. C., and Martin, A. (2019) The 26S Proteasome Utilizes a Kinetic Gateway to Prioritize Substrate Degradation, *Cell 177*, 286-+.

[45] Sloper-Mould, K. E., Jemc, J. C., Pickart, C. M., and Hicke, L. (2001) Distinct functional surface regions on ubiquitin, *J Biol Chem 276*, 30483-30489.

[46] Singh, R. K., Kazansky, Y., Wathieu, D., and Fushman, D. (2017) Hydrophobic Patch of Ubiquitin is Important for its Optimal Activation by Ubiquitin Activating Enzyme E1, *Anal Chem 89*, 7852-7860.

[47] Beal, R., Deveraux, Q., Xia, G., Rechsteiner, M., and Pickart, C. (1996) Surface hydrophobic residues of multiubiquitin chains essential for proteolytic targeting, *Proc Natl Acad Sci U S A 93*, 861-866.

[48] Yin, L., Krantz, B., Russell, N. S., Deshpande, S., and Wilkinson, K. D. (2000) Nonhydrolyzable diubiquitin analogues are inhibitors of ubiquitin conjugation and deconjugation, *Biochemistry 39*, 10001-10010.

[49] Wilkinson, K. D., Gan-Erdene, T., and Kolli, N. (2005) Derivitization of the C-terminus of ubiquitin and ubiquitin-like proteins using intein chemistry: methods and uses, *Methods Enzymol 399*, 37-51.

[50] Wang, X., Chen, C. F., Baker, P. R., Chen, P. L., Kaiser, P., and Huang, L. (2007) Mass spectrometric characterization of the affinity-purified human 26S proteasome complex, *Biochemistry 46*, 3553-3565.

[51] Leggett, D. S., Hanna, J., Borodovsky, A., Crosas, B., Schmidt, M., Baker, R. T., Walz, T., Ploegh, H., and Finley, D. (2002) Multiple associated proteins regulate proteasome structure and function, *Mol Cell 10*, 495-507.

[52] Schellenberg, M. J., Petrovich, R. M., Malone, C. C., and Williams, R. S. (2018) Selectable high-yield recombinant protein production in human cells using a GFP/YFP nanobody affinity support, *Protein Sci 27*, 1083-1092.

[53] Li, H., Carrion-Vazquez, M., Oberhauser, A. F., Marszalek, P. E., and Fernandez, J. M. (2000) Point mutations alter the mechanical stability of immunoglobulin modules, *Nat Struct Biol 7*, 1117-1120.

[54] Henderson, A., Erales, J., Hoyt, M. A., and Coffino, P. (2011) Dependence of proteasome processing rate on substrate unfolding, *J Biol Chem 286*, 17495-17502.

[55] Lu, Y., Lee, B. H., King, R. W., Finley, D., and Kirschner, M. W. (2015) Substrate degradation by the proteasome: A single-molecule kinetic analysis, *Science 348*.

[56] Thrower, J. S., Hoffman, L., Rechsteiner, M., and Pickart, C. M. (2000) Recognition of the polyubiquitin proteolytic signal, *Embo J 19*, 94-102.